

The transposable element-rich genome of the cereal pest

Sitophilus oryzae

PARISOT Nicolas^{1,§}, VARGAS-CHAVEZ Carlos^{1,2,†,§}, GOUBERT Clément^{3,4,‡,§}, BAA-PUYOLET Patrice¹, BALMAND Séverine¹, BERANGER Louis¹, BLANC Caroline¹, BONNAMOUR Aymeric¹, BOULESTEIX Matthieu³, BURLET Nelly³, CALEVRO Federica¹, CALLAERTS Patrick⁵, CHANCY Théo¹, CHARLES Hubert^{1,6}, COLELLA Stefano^{1,§}, DA SILVA BARBOSA André⁷, DELL'AGLIO Elisa¹, DI GENOVA Alex^{3,6,8}, FEBVAY Gérard¹, GABALDON Toni^{9,10,11}, GALVÃO FERRARINI Mariana¹, GERBER Alexandra¹², GILLET Benjamin¹³, HUBLEY Robert¹⁴, HUGHES Sandrine¹³, JACQUIN-JOLY Emmanuelle⁷, MAIRE Justin^{1,–}, MARCET-HOUBEN Marina⁹, MASSON Florent^{1,£}, MESLIN Camille⁷, MONTAGNE Nicolas⁷, MOYA Andrés^{2,15}, RIBEIRO DE VASCONCELOS Ana Tereza¹², RICHARD Gautier¹⁶, ROSEN Jeb¹⁴, SAGOT Marie-France^{3,6}, SMIT Arian F.A.¹⁴, STORER Jessica M.¹⁴, VINCENT-MONEGAT Carole¹, VALLIER Agnès¹, VIGNERON Aurélien^{1,#}, ZAIDMAN-REMY Anna¹, ZAMOUM Waël¹, VIEIRA Cristina^{3,6,*}, REBOLLO Rita^{1,*}, LATORRE Amparo^{2,15,*} and HEDDI Abdelaziz^{1,*}

¹ Univ Lyon, INSA Lyon, INRAE, BF2I, UMR 203, 69621 Villeurbanne, France.

² Institute for Integrative Systems Biology (I2SySBio), Universitat de València and Spanish Research Council (CSIC), València, Spain.

³ Laboratoire de Biométrie et Biologie Evolutive, UMR5558, Université Lyon 1, Université Lyon, Villeurbanne, France.

⁴ Department of Molecular Biology and Genetics, 526 Campus Rd, Cornell University, Ithaca, New York 14853, USA.

⁵ KU Leuven, University of Leuven, Department of Human Genetics, Laboratory of Behavioral and Developmental Genetics, B-3000, Leuven, Belgium.

⁶ ERABLE European Team, INRIA, Rhône-Alpes, France.

⁷ INRAE, Sorbonne Université, CNRS, IRD, UPEC, Université de Paris, Institute of Ecology and Environmental Sciences of Paris, Versailles, France.

⁸ Instituto de Ciencias de la Ingeniería, Universidad de O'Higgins, Rancagua, Chile.

⁹ Life Sciences, Barcelona Supercomputing Centre (BSC-CNS), Barcelona, Spain.

¹⁰ Mechanisms of Disease. Institute for Research in Biomedicine (IRB), Barcelona, Spain.

¹¹ Institut Català de Recerca i Estudis Avançats (ICREA), Barcelona, Spain.

¹² Laboratório de Bioinformática, Laboratório Nacional de Computação Científica, Petrópolis, Brazil.

¹³ Institut de Génomique Fonctionnelle de Lyon (IGFL), Université de Lyon, Ecole Normale Supérieure de Lyon, CNRS UMR 5242, Lyon, France.

¹⁴ Institute for Systems Biology, Seattle, WA, USA.

¹⁵ Foundation for the Promotion of Sanitary and Biomedical Research of Valencian Community (FISABIO), València, Spain.

¹⁶ IGEPP, INRAE, Institut Agro, Université de Rennes, Domaine de la Motte, 35653 Le Rheu, France.

[†] Present address: Institute of Evolutionary Biology (IBE), CSIC-Universitat Pompeu Fabra, Barcelona, Spain.

[‡] Present address: Human Genetics, McGill University, Montreal, QC, Canada.

[§] Present address: LSTM, Laboratoire des Symbioses Tropicales et Méditerranéennes, IRD, CIRAD, INRAE, SupAgro, Univ Montpellier, Montpellier, France.

[£] Present address: Global Health Institute, School of Life Sciences, Ecole Polytechnique Fédérale de Lausanne (EPFL), Lausanne 1015, Switzerland.

⁻ Present address: School of BioSciences, The University of Melbourne, Parkville, VIC 3010, Australia.

[#] Present address: Department of Evolutionary Ecology, Institute for Organismic and Molecular Evolution, Johannes Gutenberg University, 55128 Mainz, Germany.

^{\$} Authors contributed equally to this work.

^{*} Authors contributed equally to this work.

Corresponding authors

Prof. Cristina VIEIRA

Institution: Laboratoire de Biométrie et Biologie Evolutive, UMR5558, Université Lyon 1,

Université Lyon, Villeurbanne, France.

e-mail: cristina.vieira@univ-lyon1.fr

Dr. Rita REBOLLO

Institution: Laboratoire Biologie Fonctionnelle, Insectes et Interactions, UMR0203, INSA

Lyon, INRAE, Université Lyon, Villeurbanne, France.

e-mail: rita.rebollo@inrae.fr

Prof. Amparo LATORRE

Institution: Institute for Integrative Systems Biology, Universitat de València and Spanish

Research Council, València, Spain.

e-mail: amparo.latorre@uv.es

Prof. Abdelaziz HEDDI

Institution: Laboratoire Biologie Fonctionnelle, Insectes et Interactions, UMR0203, INSA

Lyon, INRAE, Université Lyon, Villeurbanne, France.

e-mail: abdelaziz.heddi@insa-lyon.fr

Abstract

Background

The rice weevil *Sitophilus oryzae* is one of the most important agricultural pests, causing extensive damage to cereal in fields and to stored grains. *S. oryzae* has an intracellular symbiotic relationship (endosymbiosis) with the Gram-negative bacterium *Sodalis pierantonius* and is a valuable model to decipher host-symbiont molecular interactions.

Results

We sequenced the *Sitophilus oryzae* genome using a combination of short and long reads to produce the best assembly for a Curculionidae species to date. We show that *S. oryzae* has undergone successive bursts of transposable element (TE) amplification, representing 72% of the genome. In addition, we show that many TE families are transcriptionally active, and changes in their expression are associated with insect endosymbiotic state. *S. oryzae* has

undergone a high gene expansion rate, when compared to other beetles. Reconstruction of host-symbiont metabolic networks revealed that, despite its recent association with cereal weevils (30 Kyear), *S. pierantonius* relies on the host for several amino acids and nucleotides to survive and to produce vitamins and essential amino-acids required for insect development and cuticle biosynthesis.

Conclusions

Here we present the genome of an agricultural pest beetle, which may act as a foundation for pest control. In addition, *S. oryzae* may be a useful model for endosymbiosis, and studying TE evolution and regulation, along with the impact of TEs on eukaryotic genomes.

Keywords

Coleoptera, weevil, *Sitophilus oryzae*, genome, transposable elements, endosymbiosis, immunity, evolution

Background

Beetles account for approximately 25% of known animals, with an estimated number of 400 000 described species [1–3]. Among them, Curculionidae (true weevils) is the largest animal family described, comprising about 70 000 species [1,4,5]. Despite being often associated with ecological invasion and ecosystem degradation, only three Curculionidae genomes are publicly available to date [6–8]. Among the cereal weevils, the rice weevil *Sitophilus oryzae* is one of the most important pests of crops of high agronomic and economic importance (wheat, maize, rice, sorghum and barley), causing extensive quantitative and qualitative

losses in field, stored grains and grain products throughout the world [9–11]. Moreover, this insect pest is of increasing concern due to its ability to rapidly evolve resistance to insecticides such as phosphine, a fumigant used to protect stored grains from insect pests [12–14].

Like other holometabolous insects, the life cycle of *S. oryzae* can be divided into four stages: egg, larva, pupa and adult (Figure 1). Females drill a small hole in the grain, deposit a single egg and seal it with secretions from their ovipositor. Up to six eggs can be laid daily by each female, totaling around 400 eggs over its entire lifespan [15]. Larvae develop and pupate within the grain kernel, metamorphose, and exit the grain as adults. The whole process takes on average 30 days [10]. Like many insects living on nutritionally poor diets, cereal weevils permanently associate with nutritional intracellular bacteria (endosymbionts) that supply them with nutrients that are not readily available in the grains, thereby increasing their fitness and invasive power. The endosymbiont of *S. oryzae*, the gamma-proteobacterium *Sodalis pierantonius* [16,17], is housed within specialized host cells, named bacteriocytes, that group together into an organ, the bacteriome [18]. Contrasting with most studied symbiotic insects, the association between *Sitophilus* spp. and *S. pierantonius* was established recently (less than 30 000 years ago), probably following the replacement of the ancestor endosymbiont, *Candidatus Nardonella*, in the Dryophthorinae subfamily [19,20]. As a result, contrary to long-lasting endosymbiotic associations, the genome of *S. pierantonius* is GC rich (56.06%), and its size is similar to that of free-living bacteria (4.5 Mbp) [16]. Moreover, it encodes genes involved in bacterial infection, including Type Three Secretion Systems (TTSS), as well as genes encoding Microbial Associated Molecular Patterns (MAMPs) that trigger Pattern Recognition Receptors (PRR), and are usually absent or reduced in bacteria involved in long-lasting associations [16,21,22]. Nevertheless, many features indicate that the genome of *S. pierantonius* is in a process of degradation, as it contains many pseudogenes (43% of the predicted protein-coding sequences) and a large number of mobile elements (18% of the genome size) [16,23]. Finally, it is important to note

that no other symbionts, with the exception of the familiar *Wolbachia* endosymbiont in some strains, have been described in *S. oryzae*.

In order to help unravel potential adaptive functions and features that could become the basis for identifying novel control strategies for weevils and other major insect pests, we have undertaken the sequencing, assembly and annotation of the genome of *S. oryzae*. Strikingly, the repeated fraction of *S. oryzae*'s genome (repeatome), composed mostly of transposable elements (TEs), is among the largest found to date in insects. TEs, the most versatile DNA units described to date, are sequences present in multiple copies and capable of relocating or replicating within a genome. While most observed TE insertions evolve neutrally or are slightly deleterious, there are a number of documented cases where TEs may facilitate host adaptation (for reviews see [24–26]). For instance, gene families involved in xenobiotic detoxification are enriched in TEs in *Drosophila melanogaster* [27], *Plutella xylostella* [28], a major crop pest, and *Myzus persicae*, another phytophagous insect causing significant agronomic losses [29]. TEs have also been frequently associated with insecticide-resistance in *Drosophila* species [30–32]. In addition, population genetics studies suggested that more than 84 TE copies in *D. melanogaster* may play a positive role in fitness-related traits [33], including xenobiotic resistance [32] and immune response to Gram-negative bacteria [34].

In eukaryotes, TE content varies drastically and contributes significantly to the size and organization of the genome. From TE-rich genomes as maize (85% [35]), humans (≈45% [36]), and the recently sequenced lungfish (≈90% [37]) for instance, to TE-poor genomes, as *D. melanogaster* (12-15% [38]), or *Arabidopsis thaliana* (≈10% [39]), repeatomes thrive on a high level of diversity. These drastic variations are also observed within animal clades, such as insects, where the proportion of TE ranges from 2% in the Antarctic midge (*Belgica antarctica*) to 65% in the migratory locust (*Locusta migratoria*) [40–42] and up to 75% in morabine grasshoppers (*Vandiemenella viatica* species) [43]. In addition to the overall TE content, the number of different TE families (homogeneous groups of phylogenetically related TE sequences), their size (number of copies per family) and sequence diversity are

also very high among insect species [44]. For instance, SINEs (Short INterspersed Elements) are almost absent from most insect genomes, but many lepidopterans harbor these elements [44]. In flies, Long Terminal Repeats retrotransposons (LTRs) are a staple of the *Drosophila* genus, but such TEs are nearly absent from other dipteran genomes (e.g. *Glossina brevipalpis* and *Megaselia scalaris*) [44]. Recent advances in sequencing have dramatically increased the level to which TEs can be studied across species and reveal that such variations can persist even within recently diverged groups, as observed within *Drosophila* species [45], or among *Heliconius* butterflies [46]. An increasing number of insect genomes are reported with large repeatomes (e.g. *Aedes aegypti* and *Ae. albopictus* 40-50% [47,48], *L. migratoria* 60-65% [40,41], *Dendrolimus punctatus* 56% [49], *Vandiemenella viatica* species 66-75% [43]).

Here we present the genome of *S. oryzae*, with a strong focus on the repeatome, its largest genomic compartment, spanning over $\approx 74\%$ of the assembly. *S. oryzae* represents a model system for stored grain pests, host-TE evolutionary biology, and the study of the molecular mechanisms acting at the early steps of symbiogenesis. Moreover, the features uncovered suggest that *S. oryzae* and its relatives have the potential to become a platform to study the interplay between TEs, host genomes and endosymbionts.






Results and discussion

Genome assembly and annotation

We have sequenced and assembled the genome of the rice weevil *S. oryzae* at a base coverage depth of 142X using a combination of short and long read strategies (see Methods and Additional file 1). The assembly pipeline was defined to optimize multiple criteria including gene completeness (BUSCO scores [50]) and reference-free metrics (number of

contigs, total length, N50, number of N's per 100 Kbp and the proportion of shared 100-mers between the assembly and short-reads). The karyotype of *S. oryzae* comprises 22 chromosomes [51], and the genome assembly consists of 2 025 scaffolds spanning 770 Mbp with a N50 of 2.86 Mbp, demonstrating a high contiguity compared to other Coleopteran genomes (Table 1). The assembly size is consistent with the genome size measured through flow cytometry (769 Mbp in females and 768 Mbp in males [51]). Haploid genome size estimations based on k-mer distributions of the short reads ranged from 785 Mbp (GenomeScope [52]) over 814 Mbp (gce [53]) to 818 Mbp (findGSE [54]), in agreement with the assembly size. BUSCO scores show the assembly is complete (97.9% complete and 0.7% fragmented), with a low duplication rate (1.9%). Consistent with the low duplication rate at the gene level, no significant haplotig contamination was observed. Finally, to confirm the completeness and consensus quality of *S. oryzae*'s assembly, we have firstly performed a K-mer analysis (100-mers), revealing that around 92% of the 100-mers of our assembly are covered by the 100-mers from the short reads, and secondly, 98% of the short reads were able to map to the assembly. Hence, thanks to the aforementioned statistics, *S. oryzae* is the best assembled Curculionidae genome to date [7,55,56] (Table 1). The complete analysis of gene content and function can be found in Additional files 2 and 3.

Table 1. Assembly statistics of *S. oryzae*'s genome in comparison to Curculionidae genomes and *T. castaneum*

	<i>Sitophilus oryzae</i>	<i>Rhynchophorus ferrugineus</i> [57]	<i>Hypothenemus hampei</i> [6]	<i>Dendroctonus ponderosae</i> [7]	<i>Tribolium castaneum</i> [56]
Statistics					
Order, Family	Coleoptera, Curculionidae	Coleoptera, Curculionidae	Coleoptera, Curculionidae	Coleoptera, Curculionidae	Coleoptera, Tenebrionidae
No. chromosomes	2n=22 [51]	2n=22 [58]	2n=14 [59]	2n=24 [60]	2n=20 [61]
No. scaffolds	2,025	24,005	15,896	8,188	2,149
Total length (Mb)	770	589	151	253	166
Scaffold N50 (Kb)	2,861	471.6	39	629	4,456
GC%	32.9	32.2	27.8	38.4	35.2
Gap length (Mb)	12.6	12.9	20.9	51.0	13.5

Median coverage	142x	62x	100x	443x	-
BUSCO (%)					
complete/partial/duplicated	98/99/1.9	98/99/2.5	97/98/0.3	96/97/4	99/100/0.4
No. protein-coding genes	15,057	23,413	19,222*	13,021	12,862

*All genes, no NCBI RefSeq annotation report available.

Annotation of the *Sitophilus oryzae* genome

Among the different pathways we were able to decipher in the genome of *S. oryzae*, we present here highlights of the main annotation efforts, followed by a detailed analysis of the TE content and impact on the host genome. A comprehensive analysis for each highlight is presented as Supplemental Notes in Additional file 2.

Phylome and horizontal gene transfer

Sitophilus oryzae has a high gene expansion rate when compared to other beetles. Some of the families with the largest expansions include genes coding for proteins with DNA binding motifs, potentially regulating functions specific to this clade. Olfactory receptors, antimicrobial peptides (AMPs) and P450 cytochromes were expanded as well, probably in response to their ecological niche and lifestyle. Additionally, we noticed an expansion of plant cell wall degrading enzymes that originated from horizontal gene transfer (HGT) events from both bacteria and fungi. Given the intimate relationship between *S. oryzae* and its endosymbiont, including the permanent infection of the female germline, we searched for evidence for HGT in the weevil genome possibly coming from *S. pierantonius*. Contrary to the genome of the tsetse fly *Glossina*, where at least three HGT events from *Wolbachia* have been reported [62], we were unable to pinpoint any HGT event from either the ancient endosymbiont *Nardonella*, *Wolbachia*, or the recently acquired *S. pierantonius*. A detailed description is reported in Additional file 2: Supplemental Note 1 [19,63-86], and Note 3 for digestive enzymes [56,87-107].

Global analysis of metabolic pathways

Using the CycADS [108] pipeline and Pathway Tools [109] we have generated BioCyc metabolism reconstruction databases for *S. oryzae* and its endosymbiont *S. pierantonius*. We compared *S. oryzae* metabolism to that of other arthropods available in the ArthropodaCyc [110] collection and we explored the metabolic exchanges between weevils and their endosymbionts. The metabolic reconstruction reveals that, despite its large genome for an endosymbiotic bacterium, *S. pierantonius* relies on its host for several central compounds, including alanine and proline, but also isocitrate, Inosine MonoPhosphate (IMP) and Uridine MonoPhosphate (UMP), to produce essential molecules to weevils, including the essential amino acids tryptophan, phenylalanine, lysine and arginine, the vitamins pantothenate, riboflavin and dihydropteroate as a folate precursor, as well as nicotinamide adenine dinucleotide (NAD) (Additional file 2: Supplemental Note 2). Among the amino acids listed above, phenylalanine, in particular is an essential precursor for the cuticle synthesis in emerging adults [111]. In addition, several studies have shown that *S. pierantonius* improves host fitness, including fertility, developmental time and flight capacity, in part by supplying the host with vitamins and improving its mitochondrial energy metabolism [112–114]. See Additional file 2: Supplemental Note 2 [19,20,108-110,112,113,115-120] for more information.

Development

Developmental gene regulatory networks of *D. melanogaster* and *Tribolium castaneum* were used to annotate *S. oryzae* genes with roles in signaling, embryonic patterning, oogenesis, segmentation and segment identity, organogenesis, appendage and eye development, and insect size and developmental transitions. Overall, we observed a high level of conservation in comparison to the red flour beetle *Tribolium castaneum*, a model coleopteran. When compared to *D. melanogaster*, several key coordinate group genes are absent in *T. castaneum* and *S. oryzae*, most notably the anterior group genes *bicoid* and *swallow* and the posterior group gene *oskar*. Moreover, seven developmental genes with two homologs in the

Drosophila genome are represented by a single ortholog in *T. castaneum* and *S. oryzae*. We also observed that homologs for signaling pathway ligands could not always be identified, which, given the presence of conserved receptors, is probably due to divergent primary sequence of the ligands. A detailed description is reported in Additional file 2: Supplemental Note 4 [56,121-138].

Cuticle protein genes

Among the distinctive biological features of coleopterans is the ability to generate a hard and thick cuticle that protects them against dehydration and represents the first physical barrier from infections and topical insecticide penetration. The analysis of cuticle proteins (CPs) showed that *S. oryzae* has an average number of CPs, but with an enrichment of members of the CPAP1 family. While some members of this family are known to be involved in molting and maintaining the integrity of the cuticle in *T. castaneum*, most are still uncharacterized [139,140]. Thus, these proteins might be involved in the development of specific cuticular tissues in *S. oryzae* or other weevils. The total number of CPs did not follow the taxonomy of beetles, suggesting instead that it might be an adaptation to their diverse lifestyles. For details see Additional file 2: Supplemental Note 5 [139-143].

Innate immune system

The analysis of immunity-related genes revealed that the genome of *S. oryzae* encodes the canonical genes involved in the three main antimicrobial pathways Toll, Imd and JAK-STAT, suggesting functional conservation of these pathways in cereal weevils. The conservation of the Imd pathway in the *S. oryzae* genome is of particular interest as its degradation in other symbiotic insects (*Acyrtosiphon pisum* [144], *B. tabaci* [145], or *Rhodnius prolixus* [146]) was initially correlated to their symbiotic status. The Imd pathway is not only present in *S. oryzae*, but it is also functional [147,148], and has evolved molecular features necessary for endosymbiont control [147] and host immune homeostasis [148]. Thus, not only is the Imd pathway conserved in cereal weevils, contrary to aphids and some other hemimetabolous

insects, but it seems to have been evolutionary “rewired” toward additional functions in symbiotic homeostasis [147]. A detailed description can be seen in Additional file 2: Supplemental Note 6 [41,62,144-193].

Detoxification and insecticide resistance

Fumigation using phosphine, hydrogen phosphide gas (PH₃), is by far the most widely used treatment for the protection of stored grains against insect pests due to its ease of use, low cost, and universal acceptance as a residue-free treatment [194,195]. However, high-level resistance to this fumigant has been reported in *S. oryzae* from different countries [13,196–203]. Hence, we searched for genes associated with detoxification and resistance to insecticide and more generally to toxins, including plant allelochemicals. The *S. oryzae* repertoire of detoxification and insecticide resistance genes includes more than 300 candidates, similar to what is seen in other coleopteran genomes. For more details see Additional file 2: Supplemental Note 7 [12-14,110,194-212].

Odorant receptors

One promising pest management strategy relies on modifying insect behavior through the use of volatile organic compounds that act on odorant receptors (ORs) [213,214]. ORs play a significant role in many crucial behaviors in insects by mediating host-seeking behavior, mating, oviposition, and predator avoidance [215]. Interfering with the behavior of pest insects and modulating their ability to find suitable hosts and mates has been shown to reduce population numbers, notably using plants that are capable of producing attractants and repellents [216,217]. *Sitophilus* spp. are known to use kairomones for host detection [218,219], as well as aggregation pheromones [220,221]. We annotated 100 candidate OR genes in *S. oryzae* (named SoryORs), including the gene encoding the co-receptor Orco. Of these genes, 46 were predicted to encode a full-length sequence. The global size of the SoryOR gene repertoire is in the range of what has been described in other species of the coleopteran suborder Polyphaga (between 46 in *Agrilus planipennis* and more than 300 in *T.*

castaneum) and close to the number of OR genes annotated in the closely related species *Dendroctonus ponderosae* (85 genes, [222]) (Additional file 2: Supplemental Note 8 [204, 218-242]).

Massive expansion of TE copies in the genome of *S. oryzae*

Detection and annotation of the repeatome

The repeatome represents the fraction of the genome categorized as repetitive. It encompasses TEs, satellites, tandem, and simple repeats. Eukaryotic TEs can be separated into two classes, depending on their replication mode [243]. DNA (Class II) based elements are able to directly move within a genome, and include terminal inverted repeat (TIR), Crypton, rolling-circle (RC/Helitron), and large composite elements (Maverick). Conversely, retrotransposons (Class I) have an RNA intermediate and replicate through RNA retrotranscription. Retrotransposons can be further divided into long terminal repeat (LTR), and non-LTR elements, including long and short interspersed nuclear repeat elements (LINEs and SINEs). Other retrotransposons include Penelope-like (PLEs) and DIRS-like elements. Each one of these TE orders can be further classified into specific superfamilies (as for instance Copia or Gypsy LTR elements, and hAT or Tc1/Mariner TIR elements), that may encompass hundreds of TE families, each containing thousands of copies. The intrinsic diversity of TEs complicates their identification and annotation, especially in understudied species genera.

We used multiple state-of-the-art TE detection tools, including RepeatModeler2 and EDTA [244,245], to generate consensus sequences of the TE families in *S. oryzae*. After an initial discovery step, more than 10 000 likely redundant TE families were identified by the dedicated programs; we combined their results using multiple sequence alignments and clustering (see Methods and Additional file 2: Figure S1) to reduce this number to 3 399.

After quality filtering (see methods) the final library includes a total of 3361 sequences. Due to the evolutionary distance between *S. oryzae* and other known coleopterans, the consensus sequences obtained were further classified using a thorough combination of sequence homology and structure (see Methods). The *S. oryzae* genome is among the most TE-rich insect genomes to date. Comparison of TE genomic content as given by RepeatMasker using TE libraries from RepeatModeler 2.0.1, EDTA v1.7.8 or our custom pipeline shows that traditional methods miss ~5% of TEs in spite of harboring more complexity (more total TE consensus, Table S1). Thus we conclude that our method is likely to improve the overall quality of the TE annotation.

We uncovered 570 Mbp of repeat sequences, corresponding to ~74% of the *S. oryzae* genome: ~2% of satellite sequences, simple or low-complexity repeats, and ~72% of other mobile elements, including TEs, (Figure 2A, Additional file 4). Given the limitation of the sequencing technologies, the proportion of satellites and TEs usually abundant in the heterochromatin is likely underestimated. We took advantage of a recent comparative analysis of TE content in 62 insect species [40] to contrast with the *S. oryzae* TE compartment. The *S. oryzae* genome ranks among those with the highest TE fraction observed in insects (Figure 2B and 2C). Within the largest insect order, Coleoptera, very little is known regarding TE distribution and evolution. *T. castaneum* harbors only 6% of TEs [56], *Hypothenemus hampei* contains 8.2% of TEs [6,246], while *Dichotomius schiffleri* harbors 21% [247]. The species closest to *S. oryzae*, *Rhynchophorus ferrugineus*, has a TE content of 45% [8]. Therefore, while TE content has been described to follow phylogenetic relationships in most insects [44,45] there is a large variation among the few Coleoptera species with available genomes. It is important to note that the pipeline we used to detect and annotate TEs in *S. oryzae* differs from the method implemented by Petersen and colleagues [40], as we incorporated 31 manually curated TE references for *S. oryzae*, and specifically annotated DNA/TIR elements based on their sequence structure (see Methods), increasing the annotation sensitivity.

Class II (DNA) elements dominate *S. oryzae*'s genome

The most striking feature of the genome of *S. oryzae* is the high abundance of Class II (DNA) elements ($\approx 32\%$ of the genome, $\approx 43\%$ of the TE content) (Figure 2A), which is the highest observed among all 62 insect species included in this analysis [40–42]. The most DNA transposon-rich genomes include mosquito *Culex quinquefasciatus*, and *Ae. aegypti*, harboring 25% and 20% of DNA transposon content in their genome, amounting to 54% and 36% of the total TE compartment, respectively [6]. The TE-rich grasshopper *L. migratoria* repeatome comprises only 14% of DNA transposons, while LINE retroelements (Class I) amount to 25%. Morabine grasshoppers, with up to 75% of TE content, show equivalent amounts of DNA, LINE and Helitrons [43]. Finally, among Coleoptera, a large diversity of repeatomes is observed (Figure 2C) with *A. planipennis*, *Leptinotarsa decemlineata* and *Onthophagus taurus* carrying an abundant LINE content, while *S. oryzae*, *T. castaneum* and *Anoplophora glabripennis* show larger DNA transposon content.

Among the Class II elements present in *S. oryzae*, the majority belongs to the TIR subclass but has not been assigned a known superfamily (Figure 2D), while Tc Mariner make up $\approx 6\%$ of DNA elements. Among the consensus sequences we were able to assemble from 5'TIR to 3'TIR (highest confidence, see Methods), the length distribution shows a continuum starting at a couple of hundred bases to a maximum of ~ 5 Kbp (see Figure 2E). We hypothesize that most of the smaller TIR families observed are miniature inverted repeat elements (MITEs). MITEs are non-autonomous elements, deriving from autonomous Class II/TIR copies, comprising two TIRs flanking a unique, non-coding, region (sometimes absent) of variable length. While the TE detection pipeline used was able to detect and annotate most Class II/TIR elements based on transposase homologies, we also specifically searched for non-autonomous TIR sequences, allowing the detection of putative MITEs that lack protein coding regions (Additional file 2: Figure S1). Among all Class II/TIR superfamilies, TIR length varies between tens of base pairs to ≈ 1 Kbp (Figure 2E). We identified short elements, composed mostly of their TIR sequences (Figure 2E), typical of

MITEs. Interestingly, the unknown TIR families show an average size smaller than 1 Kbp, while TIRs with an annotated superfamily, show larger sizes (Additional file 2: Figure S3), suggesting that most unknown families could be indeed non-autonomous MITEs. MITE size ranges were previously described from around 100 bp to copies reaching more than 1 Kbp [248]. Finally, the distribution of the proportions of TIR relative to the consensus length appears superfamily-specific (Figure 2E and Additional file 2: Figure S3), and unknown families recapitulate these patterns. In conclusion, while most unknown TIR families seem to be composed of MITEs, we cannot exclude that our homology database is limited, likely missing some unknown protein domains. The most abundant TE family detected in the *S. oryzae* genome is indeed a MITE element (TE2641_SO2_FAM0704), with 10 486 genomic hits (or the equivalent of $\approx 4\ 117$ copies based on the consensus size), corresponding to 1.3% of the genome. Large fractions of MITEs were also reported in Class II-rich genomes, such as the aforementioned mosquitoes [48,249] and the invasive *Ae. albopictus* [47], but also in many plant species such as the rice *Oryza sativa* [250–252]. Among Class II elements, we have also detected Crypton (0.9% of the genome), RC/Helitrons (0.4% of the genome) and Mavericks (0.3% of the genome).

LINE elements are the second most abundant TE subclass, representing $\approx 11\%$ of the *S. oryzae* genome, among which $\approx 35\%$ are assigned to RTE elements and $\approx 22\%$ to I elements (Figure 2D). No SINE families have been detected. LTRs are rather scarce, representing only $\approx 3\%$ of the genome (Figure 2D), and the vast majority belong to the Gypsy superfamily ($\approx 30\%$). Another retrotransposon order detected are Penelope (PLEs), reaching nearly 2% of *S. oryzae*'s genome, and DIRS (Tyrosine recombinase retrotransposons, 0.14% of the genome).

Finally, around 22% of the genome is composed of repeats for which our pipeline could not assign a known TE class (Figure 2D). CDD search on peptides greater than 100 aa extracted from “Unknown” consensus found a total of 74 distinct hits ($P \leq 0.01$), for a total of 50 consensus. We identified 14 unknown consensus with hits against known TE domains or viral sequences. The other 36 sequences had significant hits against Eukaryotic or

Prokaryotic domains, traditionally not associated with TEs. Therefore, potential non-TE sequences within the unknown fraction represent an estimated total of 0.35% of the genome and were removed from the TE library. These unknown families highlight the wealth and diversity of TEs among insects and Coleopteran genomes in particular.

TE copies make up most of non-coding sequences of *S. oryzae*'s genome

TE copies are interspersed around the *S. oryzae* genome. TEs are less frequently found close to gene transcription start sites (TSS), 5' and 3' untranslated regions (5' and 3' UTRs) and exons (Figure 3A), as expected. On the contrary, introns and intergenic sequences harbor the highest TE content (Figure 3A), amounting to around 50% of TE density, close to the general TE proportion in the genome (72%), suggesting that most non-coding DNA sequences in the *S. oryzae* genome are virtually made of TEs. To grasp the impact of TEs on intron size, we compared intron length in *S. oryzae* with two very well assembled genomes: *D. melanogaster* with a very compact and small genome, and the large, TE-rich human genome (Figure 3B). In *D. melanogaster*, introns are small and harbor few TEs, while in humans, introns are much larger potentially due to high TE accumulation [253]. *S. oryzae* intron sizes also seem to be due, at least partly, to TE accumulation. Interestingly, the *S. oryzae* genome presents a bimodal distribution, with a large proportion of small introns, as found in *D. melanogaster*, but also a noticeable amount of larger, TE packed and more human-like introns. This could suggest that specific regions of the genome could be more prone to TE elimination, and be associated with high rates of recombination and/or signature of purifying selection.

TE activity inferred by evolutionary history

Within reconstructed TE families, nucleotide substitution levels (Kimura 2 Parameters, K2P) between copies and their consensus sequences allowed estimation of their relative ages and identified potentially active ones (Figure 4A). Such "TE landscapes" are extremely helpful to pinpoint potential TE amplifications (modes in the distribution) and extinctions (valleys) within

the 0-30% K2P range (beyond, the increased divergence between copies affects negatively the sensitivity of the alignments, such that TE-derived sequences are no longer recognisable). The landscape analysis revealed a heterogeneous distribution of the TE copy divergence to their consensus within and between the main TE subclasses (Figure 4A). Most identified TE copies have a K2P divergence under 10, which is often observed in insects, and strikingly distinguishes itself from TE-rich mammalian genomes (RepeatMasker.org, [40]). While *S. oryzae*'s TE density and distribution evokes the architecture of mammalian genomes, this relatively younger TE landscape suggests higher deletion rates, and possibly a higher TE turnover rate, as observed in *Drosophila* [254,255]. LINEs and DNA transposons have the wider spectrum of divergence levels, suggesting an aggregation of distinct dynamics for the TE families present in *S. oryzae*. By contrast, the rare LTR copies identified appear to be the most homogeneous within families, with only a few substitutions between copies and their consensuses, suggesting a very recent amplification in this subclass. Finally, unknown TEs share a large part of their K2P distribution with TIR elements, though relatively less divergent from their consensus sequences as a whole. A breakdown of the K2P distributions at the superfamily level reveals specific evolutionary dynamics (Figure 4B). Diverse superfamilies, such as Tc-Mar and hAT (TIR) or RTE (LINE), show more uniform distributions, suggesting sustained activity of some of its members throughout *S. oryzae*'s genome evolution, though this could also indicate that these subfamilies could be subdivided further. As observed at the class level, all three identified LTR superfamilies (Pao, Gypsy and Copia) show families within the lowest K2P range.

TEs are transcriptionally active in somatic and germline tissues

The TE K2P landscape suggests that LTR elements as well as some LINE families and several Class II subclasses are among the youngest, and thus potentially active. In order to estimate the transcriptional activity of *S. oryzae*'s TE families, we have produced somatic (midgut) and germline (ovary) transcriptomic data. While germline tissues allow identification

of potential TE families capable of producing vertically transmitted new copies, TE derepression in somatic tissues represents the potential mutational burden due to TEs. The expression of TE families varied extensively within a class and the proportion of transcriptionally active/inactive TE families between classes was also distinct (Figure 5A). In total, 1 594 TE families were differentially expressed between ovary and midgut tissues (Figure 5B, Additional file 5); of which 329 have an absolute Log2 fold change higher than 2 (71 downregulated and 258 upregulated in midgut). In total, we detected 360 TE families downregulated in midgut when compared to ovaries: A much larger set of upregulated TE families was detected in midgut when compared to ovaries (1 236), illustrating the tighter regulation of TE copies in germline tissues. Moreover, the distribution of Log2 fold changes were similar between TE subclasses but different for LTRs, which had a higher proportion of upregulated TE families in ovaries compared to other classes (Figure 5C. Kruskal and Wallis rank-sum test: $H = 36.18$, $P < 0.01$; LTR vs. LINE, Class II or Unknown: Dunn's test: $P\text{-adj} < 0.01$). In conclusion, the large TE compartment in *S. oryzae* shows abundantly expressed TE families, and tissue-specific expression patterns.

To estimate the TE transcriptional load imposed on *S. oryzae*, we computed the percentage of total RNA-seq poly-A enriched reads mapping to TE consensus sequences in gut and ovaries (Additional file 2: Figure S4). Around 5% of the midgut transcriptome corresponds to TE sequences, while such reads represent only ~2% of ovarian transcriptomes, reinforcing the tighter regulation of TEs in germ tissues. We compared such transcriptional burden to a TE-poor (*D. melanogaster*, ~12%) and a TE-rich (*Ae. albopictus* ~50%) genome, using similar technology in equivalent tissues (adult midgut, see Methods).

It is important to note that, despite being a TE-poor genome, *D. melanogaster* harbors many young LTR elements that have been recurrently shown to transpose [256]. We did not detect a direct correlation between genomic TE content and TE expression (Additional file 2: Figure S4). *S. oryzae* bears the highest proportion of RNAseq reads mapped against TE consensus sequences (~5%), followed by *D. melanogaster* (~1%) and *Ae. albopictus* (~0.01%).

Henceforth, not only is *S. oryzae* a TE-rich genome, but the transcriptional load from TEs is higher than in other TE-rich genomes (*Ae. albopictus*), and in genomes harboring young and active TE copies (*D. melanogaster*, [38,257]).

Finally, it is important to note that while transcriptional activation of TE copies may have an impact on the host genome, it does not indicate high transposition and therefore higher mutation rates. The high transcriptional load of *S. oryzae* compared to other species might stem from differences in TE regulation. In insects, TEs are mainly silenced by small RNAs and repressive chromatin marks [258]. More specifically, piwi-interacting RNAs (piRNAs) are able to target post-transcriptional repression of TEs, and guide chromatin silencing complexes to TE copies [258–260]. Therefore, we have annotated genes implicated in small RNA biogenesis and found that all three pathways (piRNAs but also microRNAs and small interfering RNAs biogenesis pathways) are complete (Additional file 2: Supplemental Note 9). Genes involved in piRNA biosynthesis are expressed mainly in ovaries and testes, while somatic tissues (midgut) show smaller steady-state levels (Additional file 2: Supplemental Note 9 [41,94,258,259,261-282]), suggesting the piRNA pathway is potentially functional in *S. oryzae* ovaries, and could efficiently reduce transposition.

TE content is variable among *Sitophilus* species

Cereal weevils are part of the Dryophthoridae family that includes more than 500 species. Very little is known about genome dynamics in this massive phylogenetic group, and *Sitophilus* species divergence is estimated to the Neogene (2.5-25 Ma) [284]. Because of the unusual high TE copy number and landscape observed in *S. oryzae*, we analyzed three other closely related species namely *Sitophilus zeamais*, *Sitophilus granarius* and *Sitophilus linearis*. We produced low coverage sequencing and estimated the TE content from raw reads using our annotated *S. oryzae* TE library with dnaPipeTE [47]. Remarkably, among *Sitophilus* species, repeat content is variable (Figure 6A), with *S. linearis* harboring the smaller repeat load (~54%) compared to *S. oryzae* (~80%), *S. zeamais* (~79%), and *S. granarius* (~65%). Most importantly, Class II (DNA) elements of *S. oryzae* are nearly absent

from *S. linearis*, and no recent burst of LTR elements is observed, contrary to the other *Sitophilus* species, suggesting alternative TE evolutionary histories (Figure 6B). It is important to note that our analysis is biased towards *S. oryzae*, as the library used to annotate the TEs in the other *Sitophilus* species stems from automatic and manual annotation of the *S. oryzae* genome.

Overall, the comparison of TE content in closely related species highlights the influence of phylogenetic inertia, but reveals a possible TE turnover in the *S. linearis* lineage. In addition to the regulation mechanisms that strongly contribute to TE amount and variation, TE accumulation is conditioned by the drift/selection balance in populations. Indeed, effective population size has been suggested to be a major variable influencing TE content, as small, inbred or expanding populations suffer drift, allowing detrimental insertions to stay in the gene pool and thus favor TE fixation [285]. Such hypotheses should be addressed in the future, especially on recently sequenced TE-rich but rather small (<1 Gbp) genomes such as *S. oryzae*.

Endosymbionts might impact TE transcriptional regulation

The four *Sitophilus* species studied have different ecologies. *S. oryzae* and *S. zeamais* infest field cereals and silos, while *S. granarius* is mainly observed in cereal-containing silos. *S. linearis*, however, lives in a richer environment, *i.e.* tamarind seeds. In association with their diets, the interaction of *Sitophilus* species with endosymbiotic bacteria differs: the cereal weevils (*S. oryzae*, *S. zeamais* and *S. granarius*) harbor the intracellular gram-negative bacteria *S. pierantonius*, albeit at very different loads. While *S. oryzae* and *S. zeamais* show high bacterial load, *S. granarius* has a smaller bacterial population [111]. In contrast, *S. linearis* has no nutritional endosymbionts, in correlation with its richer diet. We wondered whether the presence of intracellular bacteria impacts TE regulation, and took advantage of artificially obtained aposymbiotic *S. oryzae* animals to search for TE families differentially expressed in symbiotic versus aposymbiotic ovaries. There were 50 TE families upregulated

in symbiotic ovaries compared to artificially obtained aposymbiotic ones, while 15 families were downregulated (Figure 7 and Additional file 5). Only three families presented an absolute Log2 fold change higher than 2: one LINE and two LTR/Gypsy elements. The three of them were upregulated both in symbiotic *versus* aposymbiotic ovaries, and in ovaries *versus* midgut (Additional file 5), suggesting that such elements have tissue specificity, and their expression is modulated by the presence of intracellular bacteria. Such TE families would be ideal candidates to further study the crosstalk between host genes, intracellular bacteria and TE transcriptional regulation. It is important to note that the process used to obtain aposymbiotic insects relies in heat treatments that could impact overall transcriptional regulation, and henceforth, the TEs differentially expressed between symbiotic and aposymbiotic ovaries could stem from such treatment and not from the lack of endosymbionts. In order to confirm the link between intracellular bacteria and TE regulation, it is mandatory to deplete insects of their endosymbionts using other methods, as antibiotic treatment, and reassess TE expression in aposymbiotic individuals.

Conclusion

The success of obtaining a TE-rich genome assembly complete enough to understand genome architecture and regulatory networks relies on the use of multiple sequencing platforms [286]. Here, we describe the first assembly of the repeat-rich (74%) *S. oryzae* genome, based on a combination of long and short read sequencing, and a new assembly method, WENGAN [287]. While this first assembly reaches quality standards similar to other coleopteran species (Table 1), it is important to stress that new sequencing methods have emerged in order to improve genome assemblies, including linked-reads and optical mapping [286].

We uncovered around 74% of repeated sequences in the *S. oryzae* genome, mostly TE families. While the TE landscape is marked by a wealth of Class II elements, especially non-autonomous MITE elements, ~21% of the genome is composed of unknown repeats. Large

duplicated gene families can be present in such a category, but it is tempting to speculate that the majority is composed of novel Class II elements. Indeed, Unknown and TIR elements share the same K2P landscapes, and many Class II elements have only been detected through an inverted repeat search for TIRs, and not proteins, excluding therefore TE copies old enough that TIRs are too divergent to be recognized. Moreover, we have shown that many TE families in *S. oryzae* are present in the transcriptome, suggesting that several families can be transcriptionally active. How such TE families are able to escape host silencing remains unknown. It seems obvious today that insect models such as *D. melanogaster* only represent a small window on the complex biology and evolution of TEs, and the sequencing and annotation of species with high TE content -- while challenging [288] -- is key to understanding how genomes, their size, their structure and their function evolve. In conclusion, *S. oryzae* constitutes an excellent model to understand TE dynamics and regulation and the impact on genome function.

Sitophilus species not only differ in their TE landscape, but also in their ecology and as a consequence, their association with intracellular bacteria. Comparison of TE content within the *Sitophilus* genus shows variable TE amount and diversity. In addition, intracellular bacterium impacts transcription of specific TE families in ovaries. The molecular mechanisms behind the co-evolution between an insect, its endosymbiotic bacterium and TEs remains unexplored. The impact of intracellular bacteria on host genomes is poorly studied, and the *Sitophilus* genus offers a simpler experimental setting, with a single intracellular bacterium present within specific host cells [19,112], and a well established knowledge of host-bacteria interaction [111,147,148,193,289].

Methods

DNA extraction and high-throughput sequencing

Individuals of both sexes of *S. oryzae* were reared on wheat grains at 27.5 °C with 70% relative humidity. The aposymbiotic strain was obtained by treating the symbiotic strain during one month at 35 °C and 90% relative humidity as previously described [290]. This strain is viable, fertile and was raised in the same conditions as the symbiotic strain. The aposymbiotic status was confirmed by PCR and histology. Male and female adults of *S. oryzae* were used for DNA extraction. Only the gonads were used to minimize DNA contamination from its diet, which could be still present in the gut. The reproductive organs were obtained from aposymbiotic adults and a DNA extraction protocol specific for *Sitophilus* weevils was performed. DNA extractions were performed using a STE buffer (100 mM NaCl, 1 mM Na₂EDTA pH 8, 10 mM Tris HCl pH 8). Tissues were homogenized in STE buffer, then treated successively by SDS 10%, proteinase K and RNase. Briefly, genomic DNA was purified by two successive extractions with phenol:chloroform:isoamyl alcohol (25/24/1) followed by extraction with 1 vol of chloroform:isoamyl alcohol (24/1). Genomic DNA was then precipitated by 0.7 vol isopropanol. After washing the pellet with 70% ethanol, genomic DNA was recovered in TE (1 mM EDTA, 10 mM Tris HCl pH8) buffer. Using this protocol, we obtained six different DNA samples: four from males and two from females. Each sample corresponds to the genomic DNA from 20 individuals. Five additional DNA samples were obtained using a high molecular weight DNA extraction protocol consisting of a single phenol:chloroform:isoamyl alcohol (25/24/1) extraction step from the genomic DNA of 100 males. The DNA concentration in each of these samples was quantified using a NanoDrop spectrophotometer (ThermoFisher Scientific, Waltham, MA, USA).

Sequencing was performed using a combination of Illumina, PacBio and Nanopore technologies (Additional file 1). For each sex, two Illumina libraries were generated: one paired-end library with an average fragment size of 500 bp and one mate pair library with an

average fragment size of 5 Kbp. The libraries were sequenced using an Illumina HiSeq 2000 platform with the V3 chemistry and a read size of 101 bp; the paired-end (PE) libraries were sequenced at the "Génomique & Microgénomique" service from ProfileXpert (Lyon, France) while the mate paired (MP) were sequenced at Macrogen (Seoul, South Korea). Two male samples were used to build (i) an Illumina library with an average fragment size of 200 bp which was sequenced on a HiSeq 2500 instrument using the V4 chemistry and a read size of 125 bp, and (ii) a PacBio library sequenced on seven SMRT cells using the P6-C4 chemistry. These two libraries were sequenced at KeyGene (Wageningen, The Netherlands). Finally, five male samples were used to build Nanopore libraries with the SQK-LSK109 kit and without DNA fragmentation step. The libraries were independently sequenced on five MinION R9.4 flow cells. These libraries were built and sequenced at the sequencing platform of the IGFL (Institut de Génomique Fonctionnelle de Lyon, Ecole Normale Supérieure de Lyon, France). Statistics and accession numbers from all the sequencing runs are listed in the Additional file 1.

Genome assembly and annotation

First, the Illumina reads were error-corrected using BFC release 181 [291]. The PacBio and Nanopore reads were error-corrected using LORDEC v0.9 [292] with the error-corrected Illumina overlapping PE reads, a k-mer size of 19 and solidity threshold of 3. Overlapping reads were then merged using FLASH2 v2.2 [293]. Based on the merged Illumina reads, a first short-read assembly was produced using a modified version of MINIA v3.2.1 [294] with a k-mer length of 211. A hybrid assembly was then performed using WENGAN v0.1 [287] on the MINIA short-read assembly and the raw Nanopore reads. The resulting assembly was polished using two rounds of PILON v1.23 [295] using the error-corrected Illumina overlapping PE reads and the --diploid option. A first scaffolding was then performed with two rounds of FAST-SG v06/2019 [296] and SCAFFMATCH v0.9 [297] with the error-

corrected Illumina MP, Illumina PE, PacBio and Nanopore libraries. The LR_GAPCLOSER algorithm v06/2019 [298] was used for the gap-filling step using the error-corrected PacBio and Nanopore libraries. An additional scaffolding step was performed using RASCAF v1.0.2 [299] with the available RNA-seq libraries from the Sequence Read Archive (SRX1034967-SRX1034972 and SRX3721133-SRX3721138). The resulting scaffolds were then gap-filled using a new round of LR_GAPCLOSER as previously described followed by two rounds of SEALER v2.1.5 [300] using the error-corrected Illumina overlapping PE reads and k-mer sizes of 64 and 96. Two rounds of PILON, as previously described, were performed to produce the final assembly. During the assembly process, we assessed haplotig contamination by using purge_haplotigs [301] and purge_dups [302]. No diploid peak, nor significant haplotig contamination was observed. Quality of the assembly was assessed by computing several metrics using i) QUAST v5.0.2 [303] with a minimal contig size of 100 bp and the --large and -k options, ii) BUSCO v4.0.5 [50] using the Insecta ODB10 database and the -geno option, and iii) KMC v3.0.0 [304] to evaluate the percentage of shared 100-mers between the assembly and the merged Illumina reads. Genome size prediction was performed with GenomeScope v2.0 [52], findGSE v1.94.R [54], and gce v1.0.2 [53] based on 21-mer histograms generated by JellyFish v2.2.10 [305] on the R1 reads from error-corrected Illumina overlapping PE library.

Three contaminant scaffolds corresponding to the mitochondrial genome and an artefact were removed from the assembly prior to the annotation step. The 'NCBI *Sitophilus oryzae* Annotation Release 100' was produced using the NCBI Eukaryotic Genome Annotation Pipeline v8.2.

Low-coverage genome sequencing of other *Sitophilus* species

Twenty pairs of ovaries were dissected from *S. oryzae*, *S. zeamais*, *S. granarius* and *S. linearis* females. Ovaries were homogenized in 100 mM NaCl, 1 mM EDTA pH 8, 10 mM

Tris-HCl pH 8 using a small piston. Proteinase K digestion followed in the presence of SDS for 2 h at 55 °C with shaking and for 1 h at 37 °C with RNase A. A typical phenol chloroform extraction was then performed and genomic DNA was isopropanol precipitated. Eight whole genome sequencing libraries with a median insert size of 550 bp were constructed using the Illumina TruSeq DNA PCR-free sample preparation kit (Illumina, San Diego, CA, USA), according to manufacturer's protocols. Briefly, 2 µg of each gDNA were sheared using a Covaris M220 Focused-ultrasonicator (Covaris, Inc. Woburn, MA, USA), end-repaired, A-tailed, and adapter ligated. Library quality control was performed using the 2100 Bioanalyzer System with the Agilent High Sensitivity DNA Kit (Agilent Technologies, Santa Clara, CA, USA). The libraries were individually quantified via qPCR using a KAPA Library Quantification Kits (Kapa Biosystems, Wilmington, MA, USA) for Illumina platforms, then they were pooled together in equimolar quantities and sequenced in a MiSeq sequencing system. 2x300 paired-end reads were obtained using a MiSeq Reagent Kits (600-cycles).

TE library construction

In order to annotate the *S. oryzae* repeatome, we collected and combined cutting-edge bioinformatic tools to (i) create and (ii) classify a non-redundant library of repeated elements (Additional file 2: Figure S1). First, we separately ran RepeatModeler2 (v2.0.1) [244] and EDTA v1.7.8 [245] on the assembled genome. Together, these programs include most of the recent and long-trusted tools used to detect generic repeats, but also include specific modules, such as for LTR and TIR elements. Preliminary analyses of the *S. oryzae* genome with RepeatModeler1 [306] and dnaPipeTE (v1.3) [47] suggested a rather large fraction of Class II DNA elements with terminal inverted repeats (TIRs). Thus, MITE-Tracker [307] was incorporated in our pipeline and ran independently on the genome assembly using 1- and 2-Kbp size cutoffs to detect Class II elements harboring TIRs with high sensitivity. Following this initial step, 15 510 consensus sequences obtained from RM2, EDTA and the two runs of MITE-tracker were successively clustered using MAFFT (v6.864b) [65], Mothur (v.1.45.2)

[308], and Refiner [306] to reduce redundancy in the repeat library to a total of 2 754 consensus sequences (Additional file 2: Figure S1A, <https://github.com/clemgoub/So2>). Then, we inspected the quality of the raw library by calculating the genomic coverage of each consensus. We ran the library against the genome using RepeatMasker (v4.1.1) (52) and implemented a simple algorithm “TE-trimmer.sh” to trim or split a consensus sequence wherever the genomic support drops below 5% of the average consensus coverage (Additional file 2: Figure S1A, <https://github.com/clemgoub/So2>). To mitigate any redundancy generated by the splitting, the newly trimmed library was clustered before being re-quantified using RepeatMasker (v4.1.1) [306]. At this step, we removed any consensus under 200 bp and represented by less than the equivalent of two full-length copies (in total bp). In addition, TAREAN (RepeatExplorer2 v0.3.6) [309] was used to detect and quantify candidate satellite repeats. We obtained an *ab-initio* repeat library of 3 950 consensus sequences automatically generated (Additional file 2: Figure S1A).

To refine and improve the quality of the TE consensus sequences, we then turned it over to DFAM [310] who processed the *ab initio* library following their recent guidelines [311]. First, any sequences mostly composed of tandem repeats were removed using a custom script to remove any sequences that were greater than 80% masked and/or had a sequence less than 100 bp. To generate seed alignments for each consensus, the consensus sequences were used as a search library for RepeatMasker (v4.1.1) to collect interspersed repeats. Seed alignments in the form of stockholm files were generated using the RepeatMasker output. To extend potentially truncated elements, the instances in the stockholm file for each model were extended into neighboring flanking sequences until the alignment was below a threshold equivalent to ~3 sequences in agreement. More specifically, all sequences are extended using full dynamic programming matrices using an improved affine gap penalty (default: -28 open, -6 extension) and a full substitution matrix (default: 20 % divergence, 43 % GC background). The termination of extension occurs when the improvement by adding a further column to the multiple alignment does not exceed 27 (with default scoring system). This is equivalent to a net gain of ~3 sequences in agreement.

Following extension, the new consensus were collected and consensus sequences greater than 80% similar for 80% of their length were considered duplicates and only one consensus was kept.

Upon completion, we used RepeatMasker to quantify the improved library. We selected the top 50 elements (by abundance in the genome) represented in each of the “LTR”, “LINE”, “Class II” and “Unknown” classes for manual inspection (these categories represent the 4 most abundant classes of repeats in the *S. oryzae* genome). While most consensus sequences were correctly extended and annotated (200) we noticed some cases of over-extension with LTR (consensus doubled in size) and flagged others with non-supported fragments for further trimming (Additional file 4 | tab 1). Once our quality check completed and the sequences curated, we removed fragments with 100% identity against a previously established consensus (Additional file 4 | tab 2). The final TE library contains 3 399 sequences to classify.

The classification of the final repeat library was done in successive rounds combining homology and structure methods (Additional file 2: Figure S1B). Before the final TE library was completed, we manually curated and annotated the sequences of 31 transposable elements and satellites among the most represented in *S. oryzae*. These high-confidence references were added to the default libraries used by the following programs and Repbase v.2017 [312]. We searched for nucleotide homology using RepeatMasker (v4.1.1 [306]) with -s “-slow” search settings. Best hits were chosen based on the highest score at the superfamily level allowing non-overlapping hits of related families to contribute to the same hit. In addition we used blastx [94] to query each consensus against a curated collection of TE proteins (available with RepeatMasker), as well as those identified in the 31 manual consensus sequences. We kept the best protein hit based on the blastx score. Based on the 200 consensus sequences manually inspected (see above), we set a hit length / consensus size threshold of 0.08 (RepeatMasker) and 0.03 (blastx) to keep a hit. In our hands, these thresholds were conservative to automate the classification. As an alternate homology-based method, we also ran RepeatClassifier (RepeatModeler2, v2.0.1). Finally, because

DNA elements are often represented by non-autonomous copies (unidentifiable or absent transposase) we further used einverted to flag terminal inverted repeats located less than 100 bp of the ends of each sequence. The complete library of 3 399 consensus sequences was first annotated at the subclass level (see DFAM taxonomy: <https://dfam.org/classification/tree>) if two out of RepeatMasker, RepeatClassifier and blastx annotations agreed. Further, the same rule was applied for the superfamilies if possible. At this stage, consensus sequences without annotation by homology but with TIRs as flagged by einverted, were classified as TIR and all other sequences classified as Unknown. We further divided the subclass “DNA” into “MAV” (Mavericks), “RC” (Rolling circle/Helitron), “CRY” (Crypton) and “TIR” (terminal inverted repeats). Finally, the classifications automatically given as “Unknown” to 16/274 manually inspected consensus sequences were replaced to match the manually reported classification.

In order to remove potential multi-copy gene families which would have made their way to the TE library, we searched for non-TE conserved protein domains using NCBI’s CDD search with all peptides ≥ 100 AA extracted from the unknown repeats [313]. Significant hits ($P \leq 0.01$) against known TEs and viruses were removed and all other left consensus were removed from the TE library. In conclusion, there are 21% unknown repeats, and the number of total TE consensus sequences in *S. oryzae* is 3361. The data can be obtained from <https://doi.org/10.5281/zenodo.5128603>.

In order to assess the relevance of our custom TE analysis pipeline, we ran and compared the unfiltered outputs (out.tbl file) of RepeatMasker v4.1.1 using either the TE library produced by RepeatModeler 2.0.1, EDTA v1.7.8, or our final library. An optimized TE library should minimize the total number of consensus while being able to capture as much TE in the genome as possible. Thus we compared the total number of consensus built in each library as well as the total percent of the genome masked by each respective library.

Estimation of the repeat content

The total repeat content of the *S. oryzae* genome was analyzed using RepeatMasker (v.4.1.1) and our classified library of 3 361 consensus sequences and the following parameters: -s -gccalc -no_is -cutoff 200. The subsequent alignments were parsed with the script “parseRM.pl” [314] <https://github.com/4ureliek/Parsing-RepeatMasker-Outputs>) to remove hits overlap and statistically analyzed with R version 4.0.2.

Genomic distribution of TE copies

The distribution of TE copies across the *S. oryzae* genome was assessed using two different approaches over six different genomic regions namely TSS \pm 3 Kbp, 5' UTRs, exons, introns, 3' UTRs and intergenic regions. Briefly, the coverage of all TE copies was computed over a sliding window of 100 bp across the whole genome sequence using the makewindows and coverage tools from the bedtools package [279] and the bedGraphToBigWig UCSC gtfToGenePred tool. Then the different genomic regions were retrieved from the *S. oryzae* annotation file (GFF format) using the gencode_regions script (https://github.com/saketkc/gencode_regions) and the UCSC gtfToGenePred tool (<https://github.com/ENCODE-DCC/kentUtils>). A matrix containing the TE coverage per genomic region was generated using the computeMatrix tool from deepTools [278] and used to generate metaplots using the plotProfile tool.

TE landscapes

The relative age of the different TE families identified in the genome assembly was drawn performing a “TE-landscape” analysis on the RepeatMasker outputs. Briefly, the different copies of one TE family identified by RepeatMasker are compared to their consensus sequence and the divergence (Kimura substitution level, CpG adjusted, see RepeatMasker

webpage: <http://repeatmasker.org/webrepeatmaskerhelp.html>) is calculated. The TE landscape consists of the distribution of these divergence levels. In the end, the relative age of a TE family can be seen as its distribution within the landscape graph: “older” TE families tend to have wider and flatter distribution spreading to the right (higher substitution levels) than the “recent” TE families, which are found on the left of the graph and have a narrower distribution. TE landscapes were drawn from the RepeatMasker output parsed with the options -l of “parseRM.pl”. We report here the TE landscape at the level of the TE subclass (LINE, LTR, TIR, CRY, MAV, DIRS, PLE, RC and Unknown).

dnaPipeTE comparative analysis in *Sitophilus* species

To compare the TE content of *S. oryzae* to four related species of *Sitophilus* (*S. granarius*, *S. zeamais*, *S. linearis*) we used dnaPipeTE v.1.3 [47]. dnaPipeTE allows unbiased estimation and comparison of the total repeat content across different species by assembling and quantifying TE from unassembled reads instead of a linear genome assembly. Reads for *Sitophilus* species were produced as described above. Using our new classified library (3 390 consensus) as TE database in dnaPipeTE, we were further able to identify the phylogenetic depth of the repeat identified in *S. oryzae*.

RNA sequencing and TE expression analysis

Individuals of both sexes of *S. oryzae* were reared on wheat grains at 27.5 °C with 70% relative humidity. Ten midguts and ovaries from ten-day old adults were dissected in diethylpyrocarbonate-treated Buffer A (25 mM KCl, 10 mM MgCl₂, 250 mM Sucrose, 35 mM Tris/HCl, pH 7.5). RNA was extracted in triplicates with RNAqueous-Micro (Qiagen), following the manufacturer recommendations. Single-indexed libraries were built using the SENSE mRNA-Seq Library Prep Kit V2 (Lexogen), following the manufacturer

recommendations. Libraries were then pooled in an equimolar range and sequenced using high throughput reagents on an Illumina NextSeq 500 (86 bp in single end). Raw sequencing reads were deposited at SRA archive BioProject PRJNA746240. Adapter sequences and low quality reads were filtered out with Trimmomatic (v0.36) [315] and clean reads were aligned to the *S. oryzae* genome with STAR aligner (v2.5.4b, [316]) and featureCounts from subread package [317] to obtain gene counts. We also used the STAR aligner in single-end mode to map the clean reads against all TE copies extracted from the genome with the following options: `--outFilterMultimapNmax 100 --winAnchorMultimapNmax 100 --outMultimapperOrder Random --outSAMmultNmax 1`. The mapped bam files were used as input to TETools software [318] to determine TE family expression. Genes and TE family counts were used as input for DESeq2 package (v1.30) [319] to determine differential TE expression between Ovary vs Gut tissues as well as Ovaries from symbiotic and aposymbiotic weevils. Differentially expressed TEs were defined whenever the adjusted p-value was smaller than 0.05 and Log2 fold change was higher than 1 or smaller than -1. We used the aforementioned STAR alignment parameters to map transcriptomic sequencing reads from midgut and ovaries of *S. oryzae* (Accession: SRX1034971, SRX1034972, and reads from this study deposited under the BioProject ID PRJNA746240), *D. melanogaster* (Accession: SRX029389, and SRX045361), and *Ae. albopictus* (Accession: SRX1512976, SRX1898481, SRX1898483, SRX1898487, SRX3939061, and SRX3939054) against the TE consensus sequences for each species.

List of abbreviations

AMPs: AntiMicrobial Peptides

CPs: cuticle proteins

HGT: horizontal gene transfer

IMP: Inosine MonoPhosphate

K2P: Kimura 2 Parameters

LINE: long INterspersed Element

LTR: Long Terminal Repeat

MAMPs: Microbial Associated Molecular Patterns

MITEs: miniature inverted repeat elements

ORs: odorant receptors

PRR: Pattern Recognition Receptors

PLE: Penelope-like

RC: rolling circle

SINE: Short INterspersed Element

TIR: terminal inverted repeat

TSS: transcription start sites

TEs: transposable elements

TTSS: Type Three Secretion Systems

UTR: untranslated regions

UMP: Uridine MonoPhosphate

Declarations

Ethics approval and consent to participate

Not applicable

Consent for publication

Not applicable

Availability of data and materials

Data generated and analyzed during this study are included in the published article, its additional files and publicly available repositories. This Whole Genome Shotgun project has been deposited at DDBJ/ENA/GenBank under the accession PPTJ000000000 [320]. The version described in this paper is version PPTJ020000000. The assembly can be visualised, along with gene models and supporting data, on a dedicated genome browser (https://bipaa.genouest.org/sp/sitophilus_oryzae/). Raw reads from low coverage genome sequencing of *S. zeamais*, *S. granarius* and *S. linearis* have been deposited at NCBI Sequence Read Archive (SRA) under the BioProject accessions PRJNA647530 [321], PRJNA647520 [322] and PRJNA647347 [323] respectively. TE annotation (GFF) and consensus sequences can be found at <https://dx.doi.org/10.5281/zenodo.4570415> [324]. RNA-seq reads obtained in this manuscript were deposited under the BioProject accession PRJNA746240 [325]. Bisulfite-seq reads have been deposited at NCBI SRA, under the BioProject accession PRJNA681724 [326].

Competing interests

The authors declare that they have no competing interests.

Funding

Funding for this project was provided by the Fondation de l'Institut National des Sciences Appliquées-Lyon (INSA-Lyon), the research direction of INSA-Lyon, the Santé des Plantes

et Environnement (SPE) department at the Institut National de Recherche pour l'Agriculture, l'Alimentation et l'Environnement (INRAE), the French ANR-10-BLAN-1701 (ImmunSymbArt), the French ANR-13-BSV7-0016-01 (IMetSym), the French ANR-17-CE20_0031_01 (GREEN) and a grant from la Région Rhône-Alpes (France) to AH. RR received funding from the French ANR-17-CE20-0015 (UNLEASH) and the IDEX-Lyon PALSE IMPULSION initiative. The project was also funded by European Regional Development Fund (ERDF) and Ministerio de Ciencia, Innovación y Universidades (Spain) PGC2018-099344-B-I00 to AL, and PID2019-105969GB-I00 to AM and Conselleria d'Educació, Generalitat Valenciana (Spain), grant number PROMETEO/2018/133 to AM. CV-C was a recipient of a fellowship from the Ministerio de Economía y Competitividad (Spain) and a grant from la Région Rhône-Alpes (France).

Authors' contributions

AH and AL conceived the original sequencing project and were joined by NP, RR, CG, CVC, AM and CV who participated in the coordination of the project. AV1, CVM, EDA, JM, FM and AV2 reared the inbred lines and AV1 extracted genomic DNA and RNA that was used for library construction and sequencing. BG and SH produced and sequenced the Nanopore libraries. CG, AV1, MB, NB, CV, AG and ATRDV produced and sequenced the low-coverage Illumina libraries. NP, CVC, ADG and MFS performed the genome assembly and automated gene prediction. CVC, MMH and TG analyzed and wrote the *phylome and horizontal gene transfer* note. PBP, GF, SC, HC and FC analyzed and wrote the *global analysis of metabolic pathways* note. NP analyzed and wrote the *digestive enzymes* and the *detoxification and insecticide resistance* notes. PC analyzed and wrote the *development* note. CV-C analyzed and wrote the *cuticle protein genes* note. CVM, CVC, NP, JM, LB, AB, WZ, FM, AV2 and AZR analyzed and wrote the *innate immune system* note. NM, CM, ADSB and EJJ analyzed and wrote the *odorant receptors* note. TC, CB, AV1 and RR produced the data for the

epigenetic pathways note. TC, CB, AV1, GR, CVC, CV and RR, analyzed and wrote the *epigenetic pathways* note. MGF, CG, EDA, RR, SB, GF, NM, CVM and NP produced the figures. CG, RR, JMS, JR, RH and AFAS annotated and analyzed the TE content while MGF analyzed the TE RNAseq data. NP, CVC, CG, CV, RR, AL and AH wrote the manuscript. All authors read and approved the final manuscript.

Acknowledgments

The authors acknowledge supercomputing resources made available by the Rhône-Alpes Bioinformatics center (PRABI-AMSB, <http://www.prabi.fr>) to perform the NGS data analyses. The authors would like to thank S. Robin, F. Legeai and A. Bretaudeau at the INRAE Bioinformatics Platform for Agro-ecosystems Arthropods (BIPAA) (<https://bipaa.genouest.org>) for the *S. oryzae* genome integration. The authors would like to thank F. Barbet, S. Croze and N. Nazaret from profileXpert for Illumina sequencing of *Sitophilus oryzae* libraries. The authors thank the network REacTION and its coordinators (N. Ponts, G. Le Trionnaire, I. Fudal, M. Jubault), funded by INRAE-SPE, for organizing a Bisulfite-seq workshop that allowed the production of the data presented here. We also thank J.-Y. Rasplus for collecting *Sitophilus linearis* individuals from Niger. The authors would like to thank C. Feschotte at Cornell University for the support, insights and the occasional use of bioinformatic resources.

Authors' information

Alex Di Genova @digenoma

Ana Tereza R Vasconcelos @atrvincc

Anna Zaidman-Rémy @AnnaZaidmanRemy

Camille Meslin @CamilleBurgh

Carlos Vargas-Chavez @VargasChavezC

Carole Vincent-Monegat @cmonegat

Clément Goubert @clementgoubert

Elisa Dell'Aglio @Cosmicomica

Emmanuelle Jacquin-Joly @EmmaJoly8

Florent Masson @flmasson

Justin Maire @Justin_Maire

Mariana Galvao Ferrarini @MGFerrarini

Nicolas Parisot @niparisot

Rita Rebollo @rita_rebollo

Stefano Colella @StevaTravaggio

Toni Gabaldón @Toni_Gabaldon

Figure legends

Figure 1. *Sitophilus oryzae* overview. A. Life cycle of cereal weevil *Sitophilus oryzae*. The embryo develops into a larva and pupa, and metamorphoses into a young adult, exiting the grain around 3 days after metamorphosis completion. The developmental times indicated are from a rearing condition at 27 °C and 70% relative humidity. B. Photos of adult *S. oryzae*. Lower panel shows an adult exiting the grain.

Figure 2. A. Proportion of repeat content in *S. oryzae*'s genome. The majority of repeats detected in *S. oryzae* are represented by Class II (TIR) elements, LINEs (Class I), and unclassified repeats (unknown). NR: non repetitive. B. Variation of genome size and TE content in 62 insect species from [40] and *S. oryzae*. Coleopteran species are depicted in dark blue, and *S. oryzae* in light blue. *S. oryzae* is clearly a TE-rich genome. C. TE proportion across 11 insect species, including six coleoptera. In agreement with the data used for comparison [40], PLEs are included in the LINE superfamilies, DIRS in LTRs, and RC, CRY, MAV and TIR in the DNA superfamilies. NR: non repetitive. *S. oryzae* harbors the largest TE content among Coleopterans and most insect species studied to date. Within Coleoptera, there is a large variation in TE content and type, with *A. planipennis*, *L. decemlineata* and *O. taurus* carrying an abundant LINE content, while *S. oryzae*, *T. castaneum* and *A. glabripennis* show larger DNA content. Cladogram based on [327]. D. Classification of the 570 Mbs of TEs present in the *S. oryzae* genome. Most TIR families detected were not classified into known superfamilies. RTE LINE and Gypsy LTR elements are the most abundant superfamilies among retrotransposons. Around 21% of repeats in *S. oryzae*'s genome were not classified by our pipeline, and remain unknown (grey). E. Distribution of TIR length sequences (right) detected by einverted, and the internal region present between both TIRs (left) for complete consensus of TIR superfamilies (color) and unknown TIR families (grey).

Figure 3. TE distribution in *S. oryzae*'s genome. A. Density of TE copies within gene regions. TE copies are the least abundant within TSSs, 5' and 3' UTRs and exons, while introns and intergenic regions are riddled with TEs. TSS: transcription start site, UTR: untranslated regions. B. Relationship between intron length and TE per intron in *D. melanogaster* (red), *H. sapiens* (blue) and *S. oryzae* (yellow). *S. oryzae* shares characteristics of both *Drosophila* with short and TE poor introns and Humans with a significant number of large, TE-packed introns.

Figure 4. A. TE divergence landscape. Distribution of the divergence (Kimura two parameters, K2P) between TE copies and their consensus, aggregated by TE class reported in percent of the genome. The less divergent superfamilies are distributed to the left and suggest recent activity. Strikingly, most of the TE copies have less than 10% divergence to their consensus, with a large number of copies under 5% (dotted line). The distribution of the "unknown" class overlaps with the leftmost mode of the TIR distribution, suggesting that many more TIR families are yet to be described in *S. oryzae*. Strikingly, LTR elements are the least diverged altogether with the mode of the distribution on the 0-1% divergence bin. B. Mean K2P distributions within TE superfamilies. Left panel depicts Class II families, and all Class I (retrotransposons) and unknown families are on the right panel. LTR superfamilies harbor some of the least divergent TE families, suggesting that this class may host some of the youngest TE.

Figure 5. TE family expression in midguts and ovaries from *S. oryzae*. A. Log10 normalized counts in midguts and ovaries triplicates. Normalized counts show different proportions of transcriptionally active TE families in different TE classes. B. Log10 of base mean average expression of TE families in ovaries and midguts from three biological replicates. Depicted in color only TE families which had differential expression between ovary and gut tissues ($p_{adj} < 0.05$, $|\log_2FC| > 2$). Most TE families are upregulated in midguts compared to ovaries. C. Distribution of all significant ($p_{adj} < 0.05$). Log2FC depicts specifically deregulated TE classes in each tissue. LTR elements are predominantly upregulated in ovaries.

Figure 6. TE landscape across *Sitophilus* species. A. Proportion of TE per species estimated from short reads with dnaPipeTE and a custom TE library including Repbase (release 2017) and annotated TE consensus discovered in *S. oryzae*. *S. oryzae*, *S. zeamais* and *S. granarius* harbor similar TE content, while *S. granarius* presents a smaller TE load, and *S. linearis* harbors the smallest TE content and the higher proportion of unknown repeats. The proportion of unknown repeats only found by dnaPipeTE (black) increases from *S. oryzae* to *S. linearis* with the phylogenetic distance. B. Distribution of divergence values between raw reads and repeats contig assembled with dnaPipeTE (blastn) across four *Sitophilus* species. *S. oryzae* appears to share its TE landscape with *S. zeamais* and *S. granarius*, but the three species display a distinct repeatome than *S. linearis*, in spite of their phylogenetic proximity. SO2: *S. oryzae*'s TE library produced in this analysis, DPTE: DNAPipeTE TE annotation (repeats only found by dnaPipeTE).

Figure 7. Differentially expressed TE families between symbiotic and aposymbiotic *S. oryzae* ovaries. Log10 of base mean average expression of TE families in symbiotic vs aposymbiotic ovaries from two biological replicates. Depicted in color only TE families which had differential expression between both ovary types ($p_{adj} < 0.05$, $|\log_2FC| > 2$). Two LTR elements and one LINE element are upregulated ($\log_2FC > 2$) in symbiotic ovaries.

Additional files

Additional file 1: Summary of sequencing libraries produced for *S. oryzae*. (XLSX)

Additional file 2: Supplementary notes, supplementary figures, and small tables. (PDF)

Additional file 3: Large supporting tables and datasets. (XLSX)

Additional file 4: Transposable elements annotation tables. (XLSX)

Additional file 5: STAR and TEtools mapping statistics. (XLSX)

References

1. Hunt T, Bergsten J, Levkanicova Z, Papadopoulou A, John OS, Wild R, et al. A comprehensive phylogeny of beetles reveals the evolutionary origins of a superradiation. *Science* 2007;318:1913–6. <https://doi.org/10.1126/science.1146954>.
2. Stork NE, McBroom J, Gely C, Hamilton AJ. New approaches narrow global species estimates for beetles, insects, and terrestrial arthropods. *Proc Natl Acad Sci U S A* 2015;112:7519–23. <https://doi.org/10.1073/pnas.1502408112>.
3. Hammond P. Species Inventory. In: Groombridge B, editor. *Global biodiversity: Status of the Earth's living resources*. 1992. Chapman and Hall, London. p. 17–39. https://doi.org/10.1007/978-94-011-2282-5_4.
4. McKenna DD, Sequeira AS, Marvaldi AE, Farrell BD. Temporal lags and overlap in the diversification of weevils and flowering plants. *Proc Natl Acad Sci U S A* 2009;106:7083–8. <https://doi.org/10.1073/pnas.0810618106>.
5. Oberprieler RG, Marvaldi AE, Anderson RS. Weevils, weevils, weevils everywhere*. *Zootaxa* 2007;1668:491–520. <https://doi.org/10.11646/zootaxa.1668.1.24>.
6. Vega FE, Brown SM, Chen H, Shen E, Nair MB, Ceja-Navarro JA, et al. Draft genome of the most devastating insect pest of coffee worldwide: the coffee berry borer, *Hypothenemus hampei*. *Sci Rep* 2015;5:12525. <https://doi.org/10.1038/srep12525>.
7. Keeling CI, Yuen MM, Liao NY, Roderick Docking T, Chan SK, Taylor GA, et al. Draft genome of the mountain pine beetle, *Dendroctonus ponderosae* Hopkins, a major forest pest. *Genome Biol* 2013;14:R27. <https://doi.org/10.1186/gb-2013-14-3-r27>.
8. Hazzouri KM, Sudalaimuthuasari N, Kundu B, Nelson D, Al-Deeb MA, Le Mansour A, et al. The genome of pest *Rhynchophorus ferrugineus* reveals gene families important at the plant-beetle interface. *Commun Biol* 2020;3:1–14. <https://doi.org/10.1038/s42003-020-1060-8>.
9. Zunjare R, Hossain F, Muthusamy V, Jha SK, Kumar P, Sekhar JC, et al. Genetic variability among exotic and indigenous maize inbreds for resistance to stored grain weevil (*Sitophilus oryzae* L.) infestation. *Cogent Food Agric* 2016;2:1137156. <https://doi.org/10.1080/23311932.2015.1137156>.
10. Longstaff BC. Biology of the grain pest species of the genus *Sitophilus* (Coleoptera: Curculionidae): a critical review. *Prot Ecol* 1981;3:83–130.

11. Grenier A-M, Mbaiguinam M, Delobel B. Genetical analysis of the ability of the rice weevil *Sitophilus oryzae* (Coleoptera, Curculionidae) to breed on split peas. *Heredity* 1997;79:15–23. <https://doi.org/10.1038/hdy.1997.118>.
12. Champ BR, Dyte CE. FAO global survey of pesticide susceptibility of stored grain pests. *FAO Plant Protec Bull.* 1977;25(2):49-67.
13. Nguyen TT, Collins PJ, Ebert PR. Inheritance and characterization of strong resistance to phosphine in *Sitophilus oryzae* (L.). *PLoS One* 2015;10:e0124335. <https://doi.org/10.1371/journal.pone.0124335>.
14. Mills KA. Phosphine resistance: Where to now? In: Donahaye, EJ, Navarro, S and Leesch JG, editors. *Proceeding International Conference on Controlled Atmosphere and Fumigation in Stored Products*; 2000 Oct 29-Nov 3; Fresno, USA. 2000:583–91.
15. Campbell JF. Fitness consequences of multiple mating on female *Sitophilus oryzae* L. (Coleoptera: Curculionidae). *Environ Entomol* 2005;34:833–43. <https://doi.org/10.1603/0046-225X-34.4.833>.
16. Oakeson KF, Gil R, Clayton AL, Dunn DM, von Niederhausern AC, Hamil C, et al. Genome degeneration and adaptation in a nascent stage of symbiosis. *Genome Biol Evol* 2014;6:76–93. <https://doi.org/10.1093/gbe/evt210>.
17. Heddi A, Charles H, Khatchadourian C, Bonnot G, Nardon P. Molecular characterization of the principal symbiotic bacteria of the weevil *Sitophilus oryzae*: a peculiar G + C content of an endocytobiotic DNA. *J Mol Evol* 1998;47:52–61. <https://doi.org/10.1007/pl00006362>.
18. Heddi A, Charles H, Khatchadourian C. Intracellular bacterial symbiosis in the genus *Sitophilus*: the 'biological individual' concept revisited. *Res Microbiol* 2001;152:431–7. [https://doi.org/10.1016/S0923-2508\(01\)01216-5](https://doi.org/10.1016/S0923-2508(01)01216-5).
19. Lefèvre C, Charles H, Vallier A, Delobel B, Farrell B, Heddi A. Endosymbiont phylogenesis in the Dryophthoridae weevils: evidence for bacterial replacement. *Mol Biol Evol* 2004;21:965–73. <https://doi.org/10.1093/molbev/msh063>.
20. Clayton AL, Oakeson KF, Gutin M, Pontes A, Dunn DM, Niederhausern AC von, et al. A novel human-infection-derived bacterium provides insights into the evolutionary origins of mutualistic insect–bacterial symbioses. *PLoS Genet* 2012;8:e1002990. <https://doi.org/10.1371/journal.pgen.1002990>.
21. Akman L, Yamashita A, Watanabe H, Oshima K, Shiba T, Hattori M, et al. Genome sequence of the endocellular obligate symbiont of tsetse flies, *Wigglesworthia glossinidia*. *Nat Genet* 2002;32:402–7. <https://doi.org/10.1038/ng986>.
22. Shigenobu S, Watanabe H, Hattori M, Sakaki Y, Ishikawa H. Genome sequence of the endocellular bacterial symbiont of aphids *Buchnera* sp. APS. *Nature* 2000;407:81–6. <https://doi.org/10.1038/35024074>.
23. Gil R, Belda E, Gosalbes MJ, Delaye L, Vallier A, Vincent-Monégat C, et al. Massive presence of insertion sequences in the genome of SOPE, the primary endosymbiont of the rice weevil *Sitophilus oryzae*. *Int Microbiol Off J Span Soc Microbiol* 2008;11:41–8.
24. Rebollo R, Romanish MT, Mager DL. Transposable elements: an abundant and natural source of regulatory sequences for host genes. *Annu Rev Genet* 2012;46:21–42. <https://doi.org/10.1146/annurev-genet-110711-155621>.
25. Bourque G, Burns KH, Gehring M, Gorbunova V, Seluanov A, Hammell M, et al. Ten things you should know about transposable elements. *Genome Biol* 2018;19:199. <https://doi.org/10.1186/s13059-018-1577-z>.
26. Chuong EB, Elde NC, Feschotte C. Regulatory activities of transposable elements: from conflicts to benefits. *Nat Rev Genet* 2017;18:71–86. <https://doi.org/10.1038/nrg.2016.139>.
27. Chen S, Li X. Transposable elements are enriched within or in close proximity to xenobiotic-metabolizing cytochrome P450 genes. *BMC Evol Biol* 2007;7:46. <https://doi.org/10.1186/1471-2148-7-46>.
28. You M, Yue Z, He W, Yang X, Yang G, Xie M, et al. A heterozygous moth genome provides insights into herbivory and detoxification. *Nat Genet* 2013;45:220–5.

- <https://doi.org/10.1038/ng.2524>.
29. Singh KS, Troczka BJ, Duarte A, Balabanidou V, Trissi N, Paladino LZC, et al. The genetic architecture of a host shift: An adaptive walk protected an aphid and its endosymbiont from plant chemical defenses. *Sci Adv* 2020;6:eaba1070. <https://doi.org/10.1126/sciadv.aba1070>.
30. Carareto CMA, Hernandez EH, Vieira C. Genomic regions harboring insecticide resistance-associated Cyp genes are enriched by transposable element fragments carrying putative transcription factor binding sites in two sibling *Drosophila* species. *Gene* 2014;537:93–9. <https://doi.org/10.1016/j.gene.2013.11.080>.
31. Rostant WG, Wedell N, Hosken DJ. Chapter 2 - Transposable Elements and Insecticide Resistance. In: Goodwin SF, Friedmann T, Dunlap JC, editors. *Adv. Genet.*, vol. 78, Academic Press; 2012, p. 169–201. <https://doi.org/10.1016/B978-0-12-394394-1.00002-X>.
32. Mateo L, Ullastres A, González J. A Transposable element insertion confers xenobiotic resistance in *Drosophila*. *PLoS Genet* 2014;10:e1004560. <https://doi.org/10.1371/journal.pgen.1004560>.
33. Rech GE, Bogaerts-Márquez M, Barrón MG, Merenciano M, Villanueva-Cañas JL, Horváth V, et al. Stress response, behavior, and development are shaped by transposable element-induced mutations in *Drosophila*. *PLoS Genet* 2019;15:e1007900. <https://doi.org/10.1371/journal.pgen.1007900>.
34. Ullastres A, Merenciano M, González J. Regulatory regions in natural transposable element insertions drive interindividual differences in response to immune challenges in *Drosophila*. *Genome Biol* 2021;22:265. <https://doi.org/10.1186/s13059-021-02471-3>.
35. Schnable PS, Ware D, Fulton RS, Stein JC, Wei F, Pasternak S, et al. The B73 maize genome: complexity, diversity, and dynamics. *Science* 2009;326:1112–5. <https://doi.org/10.1126/science.1178534>.
36. Lander ES, Linton LM, Birren B, Nusbaum C, Zody MC, Baldwin J, et al. Initial sequencing and analysis of the human genome. *Nature* 2001;409:860–921. <https://doi.org/10.1038/35057062>.
37. Meyer A, Schloissnig S, Franchini P, Du K, Woltering JM, Irisarri I, et al. Giant lungfish genome elucidates the conquest of land by vertebrates. *Nature* 2021;1–6. <https://doi.org/10.1038/s41586-021-03198-8>.
38. Adams MD, Celniker SE, Holt RA, Evans CA, Gocayne JD, Amanatides PG, et al. The Genome Sequence of *Drosophila melanogaster*. *Science* 2000;287:2185–95. <https://doi.org/10.1126/science.287.5461.2185>.
39. The Arabidopsis Genome Initiative. Analysis of the genome sequence of the flowering plant *Arabidopsis thaliana*. *Nature* 2000;408:796–815. <https://doi.org/10.1038/35048692>.
40. Petersen M, Armisen D, Gibbs RA, Hering L, Khila A, Mayer G, et al. Diversity and evolution of the transposable element repertoire in arthropods with particular reference to insects. *BMC Evol Biol* 2019;19:11. <https://doi.org/10.1186/s12862-018-1324-9>.
41. Wang X, Fang X, Yang P, Jiang X, Jiang F, Zhao D, et al. The locust genome provides insight into swarm formation and long-distance flight. *Nat Commun* 2014;5:2957. <https://doi.org/10.1038/ncomms3957>.
42. Kelley JL, Peyton JT, Fiston-Lavier A-S, Teets NM, Yee M-C, Johnston JS, et al. Compact genome of the Antarctic midge is likely an adaptation to an extreme environment. *Nat Commun* 2014;5:4611. <https://doi.org/10.1038/ncomms5611>.
43. Palacios-Gimenez OM, Koelman J, Palmada-Flores M, Bradford TM, Jones KK, Cooper SJB, et al. Comparative analysis of morabine grasshopper genomes reveals highly abundant transposable elements and rapidly proliferating satellite DNA repeats. *BMC Biol* 2020;18:199. <https://doi.org/10.1186/s12915-020-00925-x>.
44. Gilbert C, Peccoud J, Cordaux R. Transposable elements and the evolution of insects. *Annu Rev Entomol.* 2021;66:355–372. <https://doi.org/10.1146/annurev-ento-070720->

- 074650.
45. Sessegolo C, Burlet N, Haudry A. Strong phylogenetic inertia on genome size and transposable element content among 26 species of flies. *Biol Lett* 2016;12:20160407. <https://doi.org/10.1098/rsbl.2016.0407>.
46. Ray DA, Grimshaw JR, Halsey MK, Korstian JM, Osmanski AB, Sullivan KAM, et al. Simultaneous TE analysis of 19 Heliconiine butterflies yields novel insights into rapid TE-based genome diversification and multiple SINE births and deaths. *Genome Biol Evol* 2019;11:2162–77. <https://doi.org/10.1093/gbe/evz125>.
47. Goubert C, Modolo L, Vieira C, Valiente Moro C, Mavingui P, Boulesteix M. De novo assembly and annotation of the Asian tiger mosquito (*Aedes albopictus*) repeatome with dnaPipeTE from raw genomic reads and comparative analysis with the Yellow fever mosquito (*Aedes aegypti*). *Genome Biol Evol* 2015;7:1192–205. <https://doi.org/10.1093/gbe/evv050>.
48. Nene V, Wortman JR, Lawson D, Haas B, Kodira C, Tu Z (Jake), et al. Genome sequence of *Aedes aegypti*, a major arbovirus vector. *Science* 2007;316:1718–23. <https://doi.org/10.1126/science.1138878>.
49. Zhang S, Shen S, Peng J, Zhou X, Kong X, Ren P, et al. Chromosome-level genome assembly of an important pine defoliator, *Dendrolimus punctatus* (Lepidoptera; Lasiocampidae). *Mol Ecol Resour* 2020;20:1023–37. <https://doi.org/10.1111/1755-0998.13169>.
50. Seppey M, Manni M, Zdobnov EM. BUSCO: Assessing genome assembly and annotation completeness. In: Kollmar M, editor. *Gene Prediction. Methods Mol Biol*. 2019;1962. p. 227–45. https://doi.org/10.1007/978-1-4939-9173-0_14.
51. Silva AA, Braga LS, Corrêa AS, Holmes VR, Johnston JS, Oppert B, et al. Comparative cytogenetics and derived phylogenetic relationship among *Sitophilus* grain weevils (Coleoptera, Curculionidae, Dryophthorinae). *Comp Cytogenet* 2018;12:223–45. <https://doi.org/10.3897/CompCytogen.v12i2.26412>.
52. Vurture GW, Sedlazeck FJ, Nattestad M, Underwood CJ, Fang H, Gurtowski J, et al. GenomeScope: fast reference-free genome profiling from short reads. *Bioinformatics* 2017;33:2202–4. <https://doi.org/10.1093/bioinformatics/btx153>.
53. Liu B, Shi Y, Yuan J, Hu X, Zhang H, Li N, et al. Estimation of genomic characteristics by analyzing k-mer frequency in de novo genome projects. *ArXiv13082012 Q-Bio* 2020.
54. Sun H, Ding J, Piednoël M, Schneeberger K. findGSE: estimating genome size variation within human and *Arabidopsis* using k-mer frequencies. *Bioinformatics* 2018;34:550–7. <https://doi.org/10.1093/bioinformatics/btx637>.
55. McKenna DD, Scully ED, Pauchet Y, Hoover K, Kirsch R, Geib SM, et al. Genome of the Asian longhorned beetle (*Anoplophora glabripennis*), a globally significant invasive species, reveals key functional and evolutionary innovations at the beetle-plant interface. *Genome Biol* 2016;17:227. <https://doi.org/10.1186/s13059-016-1088-8>.
56. *Tribolium* Genome Sequencing Consortium, Richards S, Gibbs RA, Weinstock GM, Brown SJ, Denell R, et al. The genome of the model beetle and pest *Tribolium castaneum*. *Nature* 2008;452:949–55. <https://doi.org/10.1038/nature06784>.
57. Dias GB, Altammami MA, El-Shafie HAF, Alhoshani FM, Al-Fageeh MB, Bergman CM, et al. Haplotype-resolved genome assembly enables gene discovery in the red palm weevil *Rhynchophorus ferrugineus*. *Sci Rep* 2021;11:9987. <https://doi.org/10.1038/s41598-021-89091-w>.
58. Al-Qahtani AH, Al-Khalifa MS, Al-Saleh AA. Karyotype, meiosis and sperm formation in the red palm weevil *Rhynchophorus ferrugineus*. *Cytologia* 2014;79:235–42. <https://doi.org/10.1508/cytologia.79.235>.
59. Brun LO, Stuart J, Gaudichon V, Aronstein K, French-Constant RH. Functional haplodiploidy: a mechanism for the spread of insecticide resistance in an important international insect pest. *Proc Natl Acad Sci U S A* 1995;92:9861–5. <https://doi.org/10.1073/pnas.92.21.9861>.
60. Lanier GN, Wood DL. Controlled mating, karyology, morphology, and sex-ratio in the

- Dendroctonus ponderosae* complex. Ann Entomol Soc Am 1968;61:517–26. <https://doi.org/10.1093/aesa/61.2.517>.
61. Stuart JJ, Mocelin G. Cytogenetics of chromosome rearrangements in *Tribolium castaneum*. Genome 1995. <https://doi.org/10.1139/g95-085>.
62. Initiative IGG. Genome sequence of the Tsetse fly (*Glossina morsitans*): Vector of African trypanosomiasis. Science 2014;344:380–6. <https://doi.org/10.1126/science.1249656>.
63. De Bie T, Cristianini N, Demuth JP, Hahn MW. CAFE: a computational tool for the study of gene family evolution. Bioinformatics 2006;22:1269–71. <https://doi.org/10.1093/bioinformatics/btl097>.
64. Edgar RC. MUSCLE: multiple sequence alignment with high accuracy and high throughput. Nucleic Acids Res 2004;32:1792–7. <https://doi.org/10.1093/nar/gkh340>.
65. Katoh K, Standley DM. MAFFT multiple sequence alignment software version 7: improvements in performance and usability. Mol Biol Evol 2013;30:772–80. <https://doi.org/10.1093/molbev/mst010>.
66. Lassmann T, Sonnhammer ELL. Kalign--an accurate and fast multiple sequence alignment algorithm. BMC Bioinformatics 2005;6:298. <https://doi.org/10.1186/1471-2105-6-298>.
67. Wallace IM, O'Sullivan O, Higgins DG, Notredame C. M-Coffee: combining multiple sequence alignment methods with T-Coffee. Nucleic Acids Res 2006;34:1692–9. <https://doi.org/10.1093/nar/gkl091>.
68. Capella-Gutiérrez S, Silla-Martínez JM, Gabaldón T. trimAl: a tool for automated alignment trimming in large-scale phylogenetic analyses. Bioinformatics 2009;25:1972–3. <https://doi.org/10.1093/bioinformatics/btp348>.
69. Nguyen L-T, Schmidt HA, von Haeseler A, Minh BQ. IQ-TREE: a fast and effective stochastic algorithm for estimating maximum-likelihood phylogenies. Mol Biol Evol 2015;32:268–74. <https://doi.org/10.1093/molbev/msu300>.
70. Huerta-Cepas J, Capella-Gutiérrez S, Pryszcz LP, Marcet-Houben M, Gabaldón T. PhylomeDB v4: zooming into the plurality of evolutionary histories of a genome. Nucleic Acids Res 2014;42:D897–902. <https://doi.org/10.1093/nar/gkt1177>.
71. Wehe A, Bansal MS, Burleigh JG, Eulenstein O. DupTree: a program for large-scale phylogenetic analyses using gene tree parsimony. Bioinformatics 2008;24:1540–1. <https://doi.org/10.1093/bioinformatics/btn230>.
72. Eddy SR. Profile hidden Markov models. Bioinformatics 1998;14:755–63. <https://doi.org/10.1093/bioinformatics/14.9.755>.
73. Al-Shahrour F, Díaz-Uriarte R, Dopazo J. FatiGO: a web tool for finding significant associations of Gene Ontology terms with groups of genes. Bioinformatics 2004;20:578–80. <https://doi.org/10.1093/bioinformatics/btg455>.
74. Huerta-Cepas J, Serra F, Bork P. ETE 3: Reconstruction, analysis, and visualization of phylogenomic data. Mol Biol Evol 2016;33:1635–8. <https://doi.org/10.1093/molbev/msw046>.
75. Paradis E, Claude J, Strimmer K. APE: Analyses of phylogenetics and evolution in R language. Bioinformatics 2004;20:289–90. <https://doi.org/10.1093/bioinformatics/btg412>.
76. R Core Team. R: A Language and environment for statistical computing. Vienna, Austria: R Foundation for Statistical Computing; 2019.
77. Chung H-R, Schäfer U, Jäckle H, Böhm S. Genomic expansion and clustering of ZAD-containing C2H2 zinc-finger genes in *Drosophila*. EMBO Rep 2002;3:1158–62. <https://doi.org/10.1093/embo-reports/kvf243>.
78. Chung H-R, Löhr U, Jäckle H. Lineage-specific expansion of the zinc finger associated domain ZAD. Mol Biol Evol 2007;24:1934–43. <https://doi.org/10.1093/molbev/msm121>.
79. Masson F, Vallier A, Vigneron A, Balmand S, Vincent-Monégat C, Zaidman-Rémy A, et al. Systemic infection generates a local-like immune response of the bacteriome organ in insect symbiosis. J Innate Immun 2015;7:290–301.

- <https://doi.org/10.1159/000368928>.
80. Reid WR, Sun H, Becnel JJ, Clark AG, Scott JG. Overexpression of a glutathione S-transferase (Mdgst) and a galactosyltransferase-like gene (Mdgt1) is responsible for imidacloprid resistance in house flies. *Pest Manag Sci* 2019;75:37–44. <https://doi.org/10.1002/ps.5125>.
81. Altincicek B, Knorr E, Vilcinskas A. Beetle immunity: Identification of immune-inducible genes from the model insect *Tribolium castaneum*. *Dev Comp Immunol* 2008;32:585–95. <https://doi.org/10.1016/j.dci.2007.09.005>.
82. Podell S, Gaasterland T. DarkHorse: a method for genome-wide prediction of horizontal gene transfer. *Genome Biol* 2007;8:R16. <https://doi.org/10.1186/gb-2007-8-2-r16>.
83. Nguyen M, Ekstrom A, Li X, Yin Y. HGT-Finder: A new tool for horizontal gene transfer finding and application to *Aspergillus* genomes. *Toxins* 2015;7:4035–53. <https://doi.org/10.3390/toxins7104035>.
84. Nakabachi A. Horizontal gene transfers in insects. *Curr Opin Insect Sci* 2015;7:24–9. <https://doi.org/10.1016/j.cois.2015.03.006>.
85. Brelsfoard C, Tsiamis G, Falchetto M, Gomulski LM, Telleria E, Alam U, et al. Presence of extensive Wolbachia symbiont insertions discovered in the genome of its host *Glossina morsitans morsitans*. *PLoS Negl Trop Dis* 2014;8:e2728. <https://doi.org/10.1371/journal.pntd.0002728>.
86. Nikoh N, Nakabachi A. Aphids acquired symbiotic genes via lateral gene transfer. *BMC Biol* 2009;7:12. <https://doi.org/10.1186/1741-7007-7-12>.
87. Pauchet Y, Wilkinson P, Chauhan R, Ffrench-Constant RH. Diversity of beetle genes encoding novel plant cell wall degrading enzymes. *PLoS One* 2010;5:e15635. <https://doi.org/10.1371/journal.pone.0015635>.
88. Rawlings ND, Barrett AJ, Thomas PD, Huang X, Bateman A, Finn RD. The MEROPS database of proteolytic enzymes, their substrates and inhibitors in 2017 and a comparison with peptidases in the PANTHER database. *Nucleic Acids Res* 2018;46:D624–32. <https://doi.org/10.1093/nar/gkx1134>.
89. Terra WR, Cristofolletti PT. Midgut proteinases in three divergent species of Coleoptera. *Comp Biochem Physiol B Biochem Mol Biol* 1996;113:725–30. [https://doi.org/10.1016/0305-0491\(95\)02037-3](https://doi.org/10.1016/0305-0491(95)02037-3).
90. Murdock LL, Brookhart G, Dunn PE, Foard DE, Kelley S, Kitch L, et al. Cysteine digestive proteinases in Coleoptera. *Comp Biochem Physiol Part B Comp Biochem* 1987;87:783–7. [https://doi.org/10.1016/0305-0491\(87\)90388-9](https://doi.org/10.1016/0305-0491(87)90388-9).
91. Liang C, Brookhart G, Feng GH, Reeck GR, Kramer KJ. Inhibition of digestive proteinases of stored grain Coleoptera by oryzacystatin, a cysteine proteinase inhibitor from rice seed. *FEBS Lett* 1991;278:139–42. [https://doi.org/10.1016/0014-5793\(91\)80102-9](https://doi.org/10.1016/0014-5793(91)80102-9).
92. Mossé J. Acides aminés de 16 céréales et protéagineux: variations et clés du calcul de la composition en fonction du taux d'azote des grain(e)s. *Conséquences nutritionnelles*. INRA Prod Anim 1990;3:103–19.
93. Lombard V, Golaconda Ramulu H, Drula E, Coutinho PM, Henrissat B. The carbohydrate-active enzymes database (CAZy) in 2013. *Nucleic Acids Res* 2014;42:D490–5. <https://doi.org/10.1093/nar/gkt1178>.
94. Camacho C, Coulouris G, Avagyan V, Ma N, Papadopoulos J, Bealer K, et al. BLAST+: architecture and applications. *BMC Bioinformatics* 2009;10:421. <https://doi.org/10.1186/1471-2105-10-421>.
95. Zhang H, Yohe T, Huang L, Entwistle S, Wu P, Yang Z, et al. dbCAN2: a meta server for automated carbohydrate-active enzyme annotation. *Nucleic Acids Res* 2018;46:W95–101. <https://doi.org/10.1093/nar/gky418>.
96. Martynov AG, Elpidina EN, Perkin L, Oppert B. Functional analysis of C1 family cysteine peptidases in the larval gut of *Tenebrio molitor* and *Tribolium castaneum*. *BMC Genomics* 2015;16:75. <https://doi.org/10.1186/s12864-015-1306-x>.
97. Schoville SD, Chen YH, Andersson MN, Benoit JB, Bhandari A, Bowsher JH, et al. A

- model species for agricultural pest genomics: the genome of the Colorado potato beetle, *Leptinotarsa decemlineata* (Coleoptera: Chrysomelidae). *Sci Rep* 2018;8:1931. <https://doi.org/10.1038/s41598-018-20154-1>.
98. Jongsma MA, Bolter C. The adaptation of insects to plant protease inhibitors. *J Insect Physiol* 1997;43:885–95. [https://doi.org/10.1016/S0022-1910\(97\)00040-1](https://doi.org/10.1016/S0022-1910(97)00040-1).
99. Ryan CA. Protease inhibitors in plants: Genes for improving defenses against insects and pathogens. *Annu Rev Phytopathol* 1990;28:425–49. <https://doi.org/10.1146/annurev.py.28.090190.002233>.
100. Sosulski FW, Minja LA, Christensen DA. Trypsin inhibitors and nutritive value in cereals. *Plant Foods Hum Nutr* 1988;38:23–34. <https://doi.org/10.1007/BF01092307>.
101. Feng GH, Richardson M, Chen MS, Kramer KJ, Morgan TD, Reeck GR. α -amylase inhibitors from wheat: Amino acid sequences and patterns of inhibition of insect and human α -amylases. *Insect Biochem Mol Biol* 1996;26:419–26. [https://doi.org/10.1016/0965-1748\(95\)00087-9](https://doi.org/10.1016/0965-1748(95)00087-9).
102. Yetter MA, Saunders RM, Boles HP. Alpha-amylase inhibitors from wheat kernels as factors in resistance to postharvest insects. *Cereal Chem*. 1979;56:243–244.
103. Agrawal S, Kelkenberg M, Begum K, Steinfeld L, Williams CE, Kramer KJ, et al. Two essential peritrophic matrix proteins mediate matrix barrier functions in the insect midgut. *Insect Biochem Mol Biol* 2014;49:24–34. <https://doi.org/10.1016/j.ibmb.2014.03.009>.
104. Tellam RL, Wijffels G, Willadsen P. Peritrophic matrix proteins. *Insect Biochem Mol Biol* 1999;29:87–101. [https://doi.org/10.1016/s0965-1748\(98\)00123-4](https://doi.org/10.1016/s0965-1748(98)00123-4).
105. McKenna DD, Shin S, Ahrens D, Balke M, Beza-Beza C, Clarke DJ, et al. The evolution and genomic basis of beetle diversity. *Proc Natl Acad Sci U S A* 2019;116:24729–37. <https://doi.org/10.1073/pnas.1909655116>.
106. Kirsch R, Gramzow L, Theißen G, Siegfried BD, Ffrench-Constant RH, Heckel DG, et al. Horizontal gene transfer and functional diversification of plant cell wall degrading polygalacturonases: Key events in the evolution of herbivory in beetles. *Insect Biochem Mol Biol* 2014;52:33–50. <https://doi.org/10.1016/j.ibmb.2014.06.008>.
107. Shen Z, Denton M, Mutti N, Pappan K, Kanost MR, Reese JC, et al. Polygalacturonase from *Sitophilus oryzae*: possible horizontal transfer of a pectinase gene from fungi to weevils. *J Insect Sci Online* 2003;3:24. <https://doi.org/10.1093/jis/3.1.24>.
108. Vellozo AF, Véron AS, Baa-Puyoulet P, Huerta-Cepas J, Cottret L, Febvay G, et al. CycADS: an annotation database system to ease the development and update of BioCyc databases. *Database* 2011;2011:bar008. <https://doi.org/10.1093/database/bar008>.
109. Karp PD, Midford PE, Billington R, Kothari A, Krummenacker M, Latendresse M, et al. Pathway Tools version 23.0 update: software for pathway/genome informatics and systems biology. *Brief Bioinform* 2019. <https://doi.org/10.1093/bib/bbz104>.
110. Baa-Puyoulet P, Parisot N, Febvay G, Huerta-Cepas J, Vellozo AF, Gabaldón T, et al. ArthropodaCyc: a CycADS powered collection of BioCyc databases to analyse and compare metabolism of arthropods. *Database* 2016;2016 baw081. <https://doi.org/10.1093/database/baw081>.
111. Vigneron A, Masson F, Vallier A, Balmand S, Rey M, Vincent-Monégat C, et al. Insects recycle endosymbionts when the benefit is over. *Curr Biol* 2014;24:2267–73. <https://doi.org/10.1016/j.cub.2014.07.065>.
112. Heddi A, Grenier A-M, Khatchadourian C, Charles H, Nardon P. Four intracellular genomes direct weevil biology: Nuclear, mitochondrial, principal endosymbiont, and Wolbachia. *Proc Natl Acad Sci U S A* 1999;96:6814–9. <https://doi.org/10.1073/pnas.96.12.6814>.
113. Grenier AM, Nardon C, Nardon P. The role of symbiotes in flight activity of *Sitophilus* weevils. *Entomol Exp Appl* 1994;70:201–8. <https://doi.org/10.1111/j.1570-7458.1994.tb00748.x>.
114. Rio RVM, Lefevre C, Heddi A, Aksoy S. Comparative genomics of insect-symbiotic

- bacteria: influence of host environment on microbial genome composition. Appl Environ Microbiol 2003;69:6825–32. <https://doi.org/10.1128/aem.69.11.6825-6832.2003>.
115. Baker JE, Woo SM. Purification, partial characterization, and postembryonic levels of amylases from *Sitophilus oryzae* and *Sitophilus granarius*. Arch Insect Biochem Physiol 1985;2:415–28. <https://doi.org/10.1002/arch.940020409>.
116. Wicker C. Differential vitamin and choline requirements of symbiotic and aposymbiotic *S. oryzae* (Coleoptera: Curculionidae). Comp Biochem Physiol A Physiol 1983;76:177–82. [https://doi.org/10.1016/0300-9629\(83\)90311-0](https://doi.org/10.1016/0300-9629(83)90311-0).
117. Heddi A, Lestienne P, Wallace DC, Stepien G. Steady state levels of mitochondrial and nuclear oxidative phosphorylation transcripts in Kearns-Sayre syndrome. Biochim Biophys Acta 1994;1226:206–12. [https://doi.org/10.1016/0925-4439\(94\)90030-2](https://doi.org/10.1016/0925-4439(94)90030-2).
118. Hernández L, Afonso D, Rodríguez EM, Díaz C. Phenolic compounds in wheat grain cultivars. Plant Foods Hum Nutr Dordr Neth 2011;66:408–15. <https://doi.org/10.1007/s11130-011-0261-1>.
119. Panfili G, Fratianni A, Irano M. Improved normal-phase high-performance liquid chromatography procedure for the determination of carotenoids in cereals. J Agric Food Chem 2004;52:6373–7. <https://doi.org/10.1021/jf0402025>.
120. Hall RJ, Thorpe S, Thomas GH, Wood AJ. Simulating the evolutionary trajectories of metabolic pathways for insect symbionts in the genus *Sodalis*. Microb Genomics 2020;6:e000378. <https://doi.org/10.1099/mgen.0.000378>.
121. Wieschaus E, Nüsslein-Volhard C. The Heidelberg screen for pattern mutants of *Drosophila*: A personal account. Annu Rev Cell Dev Biol 2016;32:1–46. <https://doi.org/10.1146/annurev-cellbio-113015-023138>.
122. Schmidt-Ott U, Lynch JA. Emerging developmental genetic model systems in holometabolous insects. Curr Opin Genet Dev 2016;39:116–28. <https://doi.org/10.1016/j.gde.2016.06.004>.
123. Schmitt-Engel C, Schultheis D, Schwirz J, Ströhlein N, Troelenberg N, Majumdar U, et al. The iBeetle large-scale RNAi screen reveals gene functions for insect development and physiology. Nat Commun 2015;6:7822. <https://doi.org/10.1038/ncomms8822>.
124. Peel AD. The evolution of developmental gene networks: lessons from comparative studies on holometabolous insects. Philos Trans R Soc Lond B Biol Sci 2008;363:1539–47. <https://doi.org/10.1098/rstb.2007.2244>.
125. Herndon N, Shelton J, Gerischer L, Ioannidis P, Ninova M, Dönitz J, et al. Enhanced genome assembly and a new official gene set for *Tribolium castaneum*. BMC Genomics 2020;21:47. <https://doi.org/10.1186/s12864-019-6394-6>.
126. Tiegs OW, Murray FV. Memoirs: The embryonic development of *Calandra oryzae*. J Cell Sci 1938;2:159–273.
127. Duncan EJ, Benton MA, Dearden PK. Canonical terminal patterning is an evolutionary novelty. Dev Biol 2013;377:245–61. <https://doi.org/10.1016/j.ydbio.2013.02.010>.
128. Sano H, Renault AD, Lehmann R. Control of lateral migration and germ cell elimination by the *Drosophila melanogaster* lipid phosphate phosphatases Wunen and Wunen 2. J Cell Biol 2005;171:675–83. <https://doi.org/10.1083/jcb.200506038>.
129. Savard J, Marques-Souza H, Aranda M, Tautz D. A segmentation gene in *Tribolium* produces a polycistronic mRNA that codes for multiple conserved peptides. Cell 2006;126:559–69. <https://doi.org/10.1016/j.cell.2006.05.053>.
130. Angelini DR, Kaufman TC. Comparative developmental genetics and the evolution of arthropod body plans. Annu Rev Genet 2005;39:95–119. <https://doi.org/10.1146/annurev.genet.39.073003.112310>.
131. Shippy TD, Brown SJ, Denell RE. *Maxillopedia* is the *Tribolium* ortholog of proboscipedia. Evol Dev 2000;2:145–51. <https://doi.org/10.1046/j.1525-142x.2000.00055.x>.
132. Angelini DR, Smith FW, Jockusch EL. Extent with modification: Leg patterning in the beetle *Tribolium castaneum* and the evolution of serial homologs. G3 2012;2:235–48. <https://doi.org/10.1534/g3.111.001537>.

133. Ober KA, Jockusch EL. The roles of *wingless* and *decapentaplegic* in axis and appendage development in the red flour beetle, *Tribolium castaneum*. *Dev Biol* 2006;294:391–405. <https://doi.org/10.1016/j.ydbio.2006.02.053>.
134. Mirth CK, Anthony Frankino W, Shingleton AW. Allometry and size control: what can studies of body size regulation teach us about the evolution of morphological scaling relationships? *Curr Opin Insect Sci* 2016;13:93–8. <https://doi.org/10.1016/j.cois.2016.02.010>.
135. Nijhout HF, Callier V. Developmental mechanisms of body size and wing-body scaling in insects. *Annu Rev Entomol* 2015;60:141–56. <https://doi.org/10.1146/annurev-ento-010814-020841>.
136. Huybrechts J, Bonhomme J, Minoli S, Prunier-Leterme N, Dombrovsky A, Abdel-Latif M, et al. Neuropeptide and neurohormone precursors in the pea aphid, *Acyrtosiphon pisum*. *Insect Mol Biol* 2010;19 Suppl 2:87–95. <https://doi.org/10.1111/j.1365-2583.2009.00951.x>.
137. Gurska D, Vargas Jentsch IM, Panfilio KA. Unexpected mutual regulation underlies paralogue functional diversification and promotes epithelial tissue maturation in *Tribolium*. *Commun Biol* 2020;3:552. <https://doi.org/10.1038/s42003-020-01250-3>.
138. Dönitz J, Schmitt-Engel C, Grossmann D, Gerischer L, Tech M, Schoppmeier M, et al. iBeetle-Base: a database for RNAi phenotypes in the red flour beetle *Tribolium castaneum*. *Nucleic Acids Res* 2015;43:D720–725. <https://doi.org/10.1093/nar/gku1054>.
139. Jasrapuria S, Arakane Y, Osman G, Kramer KJ, Beeman RW, Muthukrishnan S. Genes encoding proteins with peritrophin A-type chitin-binding domains in *Tribolium castaneum* are grouped into three distinct families based on phylogeny, expression and function. *Insect Biochem Mol Biol* 2010;40:214–27. <https://doi.org/10.1016/j.ibmb.2010.01.011>.
140. Jasrapuria S, Specht CA, Kramer KJ, Beeman RW, Muthukrishnan S. Gene families of cuticular proteins analogous to peritrophins (CPAPs) in *Tribolium castaneum* have diverse functions. *PLoS One* 2012;7:e49844. <https://doi.org/10.1371/journal.pone.0049844>.
141. Balabanidou V, Kefi M, Aivaliotis M, Koidou V, Girotti JR, Mijailovsky SJ, et al. Mosquitoes cloak their legs to resist insecticides. *Proc Biol Sci* 2019;286:20191091. <https://doi.org/10.1098/rspb.2019.1091>.
142. Arakane Y, Lomakin J, Gehrke SH, Hiromasa Y, Tomich JM, Muthukrishnan S, et al. Formation of rigid, non-flight forewings (elytra) of a beetle requires two major cuticular proteins. *PLoS Genet* 2012;8:e1002682. <https://doi.org/10.1371/journal.pgen.1002682>.
143. Ioannidou ZS, Theodoropoulou MC, Papandreou NC, Willis JH, Hamodrakas SJ. CutProtFam-Pred: detection and classification of putative structural cuticular proteins from sequence alone, based on profile hidden Markov models. *Insect Biochem Mol Biol* 2014;52:51–9. <https://doi.org/10.1016/j.ibmb.2014.06.004>.
144. Gerardo NM, Altincicek B, Anselme C, Atamian H, Barribeau SM, de Vos M, et al. Immunity and other defenses in pea aphids, *Acyrtosiphon pisum*. *Genome Biol* 2010;11:R21. <https://doi.org/10.1186/gb-2010-11-2-r21>.
145. Zhang C-R, Zhang S, Xia J, Li F-F, Xia W-Q, Liu S-S, et al. The immune strategy and stress response of the mediterranean species of the *Bemisia tabaci* complex to an orally delivered bacterial pathogen. *PLoS One* 2014;9:e94477. <https://doi.org/10.1371/journal.pone.0094477>.
146. Salcedo-Porras N, Guarneri A, Oliveira PL, Lowenberger C. *Rhodnius prolixus*: Identification of missing components of the IMD immune signaling pathway and functional characterization of its role in eliminating bacteria. *PLoS One* 2019;14:e0214794. <https://doi.org/10.1371/journal.pone.0214794>.
147. Maire J, Vincent-Monégat C, Masson F, Zaidman-Rémy A, Heddi A. An IMD-like pathway mediates both endosymbiont control and host immunity in the cereal weevil *Sitophilus* spp. *Microbiome* 2018;6:6. <https://doi.org/10.1186/s40168-017-0397-9>.

148. Maire J, Vincent-Monégat C, Balmand S, Vallier A, Hervé M, Masson F, et al. Weevil pgrp-lb prevents endosymbiont TCT dissemination and chronic host systemic immune activation. *Proc Natl Acad Sci U S A* 2019;116:5623–32. <https://doi.org/10.1073/pnas.1821806116>.
149. Sheehan G, Garvey A, Croke M, Kavanagh K. Innate humoral immune defences in mammals and insects: The same, with differences? *Virulence* 2018;9:1625–39. <https://doi.org/10.1080/21505594.2018.1526531>.
150. Strand MR. The insect cellular immune response. *Insect Sci* 2008;15:1–14. <https://doi.org/10.1111/j.1744-7917.2008.00183.x>.
151. He Y, Cao X, Li K, Hu Y, Chen Y, Blissard G, et al. A genome-wide analysis of antimicrobial effector genes and their transcription patterns in *Manduca sexta*. *Insect Biochem Mol Biol* 2015;62:23–37. <https://doi.org/10.1016/j.ibmb.2015.01.015>.
152. Lemaitre B, Hoffmann J. The host defense of *Drosophila melanogaster*. *Annu Rev Immunol* 2007;25:697–743. <https://doi.org/10.1146/annurev.immunol.25.022106.141615>.
153. De Gregorio E, Spellman PT, Rubin GM, Lemaitre B. Genome-wide analysis of the *Drosophila* immune response by using oligonucleotide microarrays. *Proc Natl Acad Sci U S A* 2001;98:12590–5. <https://doi.org/10.1073/pnas.221458698>.
154. Waterhouse RM, Kriventseva EV, Meister S, Xi Z, Alvarez KS, Bartholomay LC, et al. Evolutionary dynamics of immune-related genes and pathways in disease-vector mosquitoes. *Science* 2007;316:1738–43. <https://doi.org/10.1126/science.1139862>.
155. Zou Z, Evans JD, Lu Z, Zhao P, Williams M, Sumathipala N, et al. Comparative genomic analysis of the *Tribolium* immune system. *Genome Biol* 2007;8:R177. <https://doi.org/10.1186/gb-2007-8-8-r177>.
156. Cao X, He Y, Hu Y, Wang Y, Chen Y-R, Bryant B, et al. The immune signaling pathways of *Manduca sexta*. *Insect Biochem Mol Biol* 2015;62:64–74. <https://doi.org/10.1016/j.ibmb.2015.03.006>.
157. Arp AP, Hunter WB, Pelz-Stelinski KS. Annotation of the Asian citrus psyllid genome reveals a reduced innate immune system. *Front Physiol* 2016;7. <https://doi.org/10.3389/fphys.2016.00570>.
158. Kang X, Dong F, Shi C, Liu S, Sun J, Chen J, et al. DRAMP 2.0, an updated data repository of antimicrobial peptides. *Sci Data* 2019;6:148. <https://doi.org/10.1038/s41597-019-0154-y>.
159. Palmer WJ, Jiggins FM. Comparative genomics reveals the origins and diversity of arthropod immune systems. *Mol Biol Evol* 2015;32:2111–29. <https://doi.org/10.1093/molbev/msv093>.
160. Smith CA. Structure, function and dynamics in the mur family of bacterial cell wall ligases. *J Mol Biol* 2006;362:640–55. <https://doi.org/10.1016/j.jmb.2006.07.066>.
161. Gottar M, Gobert V, Michel T, Belvin M, Duyk G, Hoffmann JA, et al. The *Drosophila* immune response against Gram-negative bacteria is mediated by a peptidoglycan recognition protein. *Nature* 2002;416:640–4. <https://doi.org/10.1038/nature734>.
162. Choe K-M, Werner T, Stöven S, Hultmark D, Anderson KV. Requirement for a peptidoglycan recognition protein (PGRP) in Relish activation and antibacterial immune responses in *Drosophila*. *Science* 2002;296:359–62. <https://doi.org/10.1126/science.1070216>.
163. Kleino A, Silverman N. The *Drosophila* IMD pathway in the activation of the humoral immune response. *Dev Comp Immunol* 2014;42. <https://doi.org/10.1016/j.dci.2013.05.014>.
164. Park JT. Why does *Escherichia coli* recycle its cell wall peptides? *Mol Microbiol* 1995;17:421–6. https://doi.org/10.1111/j.1365-2958.1995.mmi_17030421.x.
165. Johnson JW, Fisher JF, Mobashery S. Bacterial cell-wall recycling. *Ann N Y Acad Sci* 2013;1277:54–75. <https://doi.org/10.1111/j.1749-6632.2012.06813.x>.
166. Kaneko T, Yano T, Aggarwal K, Lim J-H, Ueda K, Oshima Y, et al. PGRP-LC and PGRP-LE have essential yet distinct functions in the *Drosophila* immune response to monomeric DAP-type peptidoglycan. *Nat Immunol* 2006;7:715–23.

- <https://doi.org/10.1038/ni1356>.
167. Bosco-Drayon V, Poidevin M, Boneca IG, Narbonne-Reveau K, Royet J, Charroux B. Peptidoglycan sensing by the receptor PGRP-LE in the *Drosophila* gut induces immune responses to infectious bacteria and tolerance to microbiota. *Cell Host Microbe* 2012;12:153–65. <https://doi.org/10.1016/j.chom.2012.06.002>.
168. Neyen C, Poidevin M, Roussel A, Lemaitre B. Tissue- and ligand-specific sensing of gram-negative infection in drosophila by PGRP-LC isoforms and PGRP-LE. *J Immunol* Baltim Md 1950 2012;189:1886–97. <https://doi.org/10.4049/jimmunol.1201022>.
169. Tindwa H, Patnaik BB, Kim DH, Mun S, Jo YH, Lee BL, et al. Cloning, characterization and effect of TmPGRP-LE gene silencing on survival of *Tenebrio molitor* against *Listeria monocytogenes* infection. *Int J Mol Sci* 2013;14:22462–82. <https://doi.org/10.3390/ijms141122462>.
170. Michel T, Reichhart JM, Hoffmann JA, Royet J. *Drosophila* Toll is activated by Gram-positive bacteria through a circulating peptidoglycan recognition protein. *Nature* 2001;414:756–9. <https://doi.org/10.1038/414756a>.
171. Wang J, Song X, Wang M. Peptidoglycan recognition proteins in hematophagous arthropods. *Dev Comp Immunol* 2018;83:89–95. <https://doi.org/10.1016/j.dci.2017.12.017>.
172. Chowdhury M, Li C-F, He Z, Lu Y, Liu X-S, Wang Y-F, et al. Toll family members bind multiple Spätzle proteins and activate antimicrobial peptide gene expression in *Drosophila*. *J Biol Chem* 2019;294:10172–81. <https://doi.org/10.1074/jbc.RA118.006804>.
173. Valanne S, Wang J-H, Rämet M. The *Drosophila* Toll signaling pathway. *J Immunol* Baltim Md 1950 2011;186:649–56. <https://doi.org/10.4049/jimmunol.1002302>.
174. Muhammad A, Habineza P, Wang X, Xiao R, Ji T, Hou Y, et al. Spätzle homolog-mediated Toll-like pathway regulates innate immune responses to maintain the homeostasis of gut microbiota in the red palm weevil, *Rhynchophorus ferrugineus* Olivier (Coleoptera: Dryophthoridae). *Front Microbiol* 2020;11:846. <https://doi.org/10.3389/fmicb.2020.00846>.
175. Gupta SK, Kupper M, Ratzka C, Feldhaar H, Vilcinskas A, Gross R, et al. Scrutinizing the immune defence inventory of *Camponotus floridanus* applying total transcriptome sequencing. *BMC Genomics* 2015;16:540. <https://doi.org/10.1186/s12864-015-1748-1>.
176. Bang IS. JAK/STAT signaling in insect innate immunity. *Entomol Res* 2019;49:339–53. <https://doi.org/10.1111/1748-5967.12384>.
177. Wu Q, Patočka J, Kuča K. Insect antimicrobial peptides, a mini review. *Toxins* 2018;10. <https://doi.org/10.3390/toxins10110461>.
178. Callewaert L, Michiels CW. Lysozymes in the animal kingdom. *J Biosci* 2010;35:127–60. <https://doi.org/10.1007/s12038-010-0015-5>.
179. Mohrig W, Messner B. Lysozyme as antibacterial agent in honey and bees venom. *Acta Biol Med Ger* 1968;21:85–95.
180. Hultmark D. Insect lysozymes. *EXS* 1996;75:87–102. https://doi.org/10.1007/978-3-0348-9225-4_6.
181. Beckert A, Wiesner J, Baumann A, Pöppel A-K, Vogel H, Vilcinskas A. Two c-type lysozymes boost the innate immune system of the invasive ladybird *Harmonia axyridis*. *Dev Comp Immunol* 2015;49:303–12. <https://doi.org/10.1016/j.dci.2014.11.020>.
182. Beckert A, Wiesner J, Schmidtberg H, Lehmann R, Baumann A, Vogel H, et al. Expression and characterization of a recombinant i-type lysozyme from the harlequin ladybird beetle *Harmonia axyridis*. *Insect Mol Biol* 2016;25:202–15. <https://doi.org/10.1111/imb.12213>.
183. Brandazza A, Angeli S, Tegoni M, Cambillau C, Pelosi P. Plant stress proteins of the thaumatin-like family discovered in animals. *FEBS Lett* 2004;572:3–7. <https://doi.org/10.1016/j.febslet.2004.07.003>.

184. Anselme C, Pérez-Brocal V, Vallier A, Vincent-Monegat C, Charif D, Latorre A, et al. Identification of the Weevil immune genes and their expression in the bacteriome tissue. *BMC Biol* 2008;6:43. <https://doi.org/10.1186/1741-7007-6-43>.
185. Masson F, Moné Y, Vigneron A, Vallier A, Parisot N, Vincent-Monégat C, et al. Weevil endosymbiont dynamics is associated with a clamping of immunity. *BMC Genomics* 2015;16:819. <https://doi.org/10.1186/s12864-015-2048-5>.
186. Chung KT, Ourth DD. Viresin. A novel antibacterial protein from immune hemolymph of *Heliothis virescens* pupae. *Eur J Biochem* 2000;267:677–83. <https://doi.org/10.1046/j.1432-1327.2000.01034.x>.
187. Benoit JB, Adelman ZN, Reinhardt K, Dolan A, Poelchau M, Jennings EC, et al. Unique features of a global human ectoparasite identified through sequencing of the bed bug genome. *Nat Commun* 2016;7:10165. <https://doi.org/10.1038/ncomms10165>.
188. Kirkness EF, Haas BJ, Sun W, Braig HR, Perotti MA, Clark JM, et al. Genome sequences of the human body louse and its primary endosymbiont provide insights into the permanent parasitic lifestyle. *Proc Natl Acad Sci U S A* 2010;107:12168–73. <https://doi.org/10.1073/pnas.1003379107>.
189. Pachebat JA, van Keulen G, Whitten MMA, Girdwood S, Del Sol R, Dyson PJ, et al. Draft genome sequence of *Rhodococcus rhodnii* strain LMG5362, a symbiont of *Rhodnius prolixus* (Hemiptera, Reduviidae, Triatominae), the principle vector of *Trypanosoma cruzi*. *Genome Announc* 2013;1. <https://doi.org/10.1128/genomeA.00329-13>.
190. Rispe C, Legeai F, Nabity PD, Fernández R, Arora AK, Baa-Puyoulet P, et al. The genome sequence of the grape Phylloxera provides insights into the evolution, adaptation, and invasion routes of an iconic pest. *BMC Biol* 2020;18:90. <https://doi.org/10.1186/s12915-020-00820-5>.
191. Nishide Y, Kageyama D, Yokoi K, Jouraku A, Tanaka H, Futahashi R, et al. Functional crosstalk across IMD and Toll pathways: insight into the evolution of incomplete immune cascades. *Proc R Soc B Biol Sci* 2019;286:20182207. <https://doi.org/10.1098/rspb.2018.2207>.
192. Matetovici I, De Vooght L, Van Den Abbeele J. Innate immunity in the tsetse fly (*Glossina*), vector of African trypanosomes. *Dev Comp Immunol* 2019;98:181–8. <https://doi.org/10.1016/j.dci.2019.05.003>.
193. Login FH, Balmand S, Vallier A, Vincent-Monégat C, Vigneron A, Weiss-Gayet M, et al. Antimicrobial peptides keep insect endosymbionts under control. *Science* 2011;334:362–5. <https://doi.org/10.1126/science.1209728>.
194. Chaudhry MQ. Phosphine resistance. *Pestic Outlook* 2000;11:88–91. <https://doi.org/10.1039/B006348G>.
195. Chaudhry MQ. A review of the mechanisms involved in the action of phosphine as an insecticide and phosphine resistance in stored-product insects. *Pestic Sci* 1997;49:213–28.
196. Athié I, Gomes RAR, Bolonhezi S, Valentini SRT, De Castro MFPM. Effects of carbon dioxide and phosphine mixtures on resistant populations of stored-grain insects. *J Stored Prod Res* 1998;34:27–32. [https://doi.org/10.1016/S0022-474X\(97\)00026-X](https://doi.org/10.1016/S0022-474X(97)00026-X).
197. Rajendran S. Phosphine resistance in stored grain insect pests in India. *Proc. 7th Int. Work. Conf. Stored-Prod. Prot.*, 1998, p. 14–9.
198. Zeng L. Development and countermeasures of phosphine resistance in stored grain insects in Guangdong, China, 642–647. *Proc. Seventh Int. Work. Conf. Stored-Prod. Prot.* Eds J Zuxun Quan Yongsheng T Xianchang G Lianghua14–19 Oct. 1998 Beijing China Sichuan Publ. House Sci. Technol. Chengdu China, 1999.
199. Benhalima H, Chaudhry MQ, Mills KA, Price NR. Phosphine resistance in stored-product insects collected from various grain storage facilities in Morocco. *J Stored Prod Res* 2004;40:241–9. [https://doi.org/10.1016/S0022-474X\(03\)00012-2](https://doi.org/10.1016/S0022-474X(03)00012-2).
200. Pimentel MAG, Faroni LRD, Silva FH da, Batista MD, Guedes RNC. Spread of phosphine resistance among brazilian populations of three species of stored product insects. *Neotrop Entomol* 2010;39:101–7. <https://doi.org/10.1590/S1519->

- 566X2010000100014.
201. Nguyen TT, Collins PJ, Duong TM, Schlipalius DI, Ebert PR. Genetic conservation of phosphine resistance in the rice weevil *Sitophilus oryzae* (L.). J Hered 2016;107:228–37. <https://doi.org/10.1093/jhered/esw001>.
202. Holloway JC, Falk MG, Emery RN, Collins PJ, Nayak MK. Resistance to phosphine in *Sitophilus oryzae* in Australia: A national analysis of trends and frequencies over time and geographical spread. J Stored Prod Res 2016;69:129–37. <https://doi.org/10.1016/j.jspr.2016.07.004>.
203. Agrafioti P, Athanassiou CG, Nayak MK. Detection of phosphine resistance in major stored-product insects in Greece and evaluation of a field resistance test kit. J Stored Prod Res 2019;82:40–7. <https://doi.org/10.1016/j.jspr.2019.02.004>.
204. Mitchell AL, Attwood TK, Babbitt PC, Blum M, Bork P, Bridge A, et al. InterPro in 2019: improving coverage, classification and access to protein sequence annotations. Nucleic Acids Res 2019;47:D351–60. <https://doi.org/10.1093/nar/gky1100>.
205. El-Gebali S, Mistry J, Bateman A, Eddy SR, Luciani A, Potter SC, et al. The Pfam protein families database in 2019. Nucleic Acids Res 2019;47:D427–32. <https://doi.org/10.1093/nar/gky995>.
206. Sigrist CJA, de Castro E, Cerutti L, Cuche BA, Hulo N, Bridge A, et al. New and continuing developments at PROSITE. Nucleic Acids Res 2013;41:D344–347. <https://doi.org/10.1093/nar/gks1067>.
207. Scott JG, Wen Z. Cytochromes P450 of insects: the tip of the iceberg. Pest Manag Sci 2001;57:958–67. <https://doi.org/10.1002/ps.354>.
208. Hu F, Ye K, Tu X-F, Lu Y-J, Thakur K, Jiang L, et al. Identification and expression profiles of twenty-six glutathione S-transferase genes from rice weevil, *Sitophilus oryzae* (Coleoptera: Curculionidae). Int J Biol Macromol 2018;120:1063–71. <https://doi.org/10.1016/j.ijbiomac.2018.08.185>.
209. Kim K, Yang JO, Sung J-Y, Lee J-Y, Park JS, Lee H-S, et al. Minimization of energy transduction confers resistance to phosphine in the rice weevil, *Sitophilus oryzae*. Sci Rep 2019;9:14605. <https://doi.org/10.1038/s41598-019-50972-w>.
210. Schlipalius DI, Tuck AG, Jagadeesan R, Nguyen T, Kaur R, Subramanian S, et al. Variant linkage analysis using *de novo* transcriptome sequencing identifies a conserved phosphine resistance gene in insects. Genetics 2018;209:281–90. <https://doi.org/10.1534/genetics.118.300688>.
211. Haddi K, Valbon WR, Viteri Jumbo LO, de Oliveira LO, Guedes RNC, Oliveira EE. Diversity and convergence of mechanisms involved in pyrethroid resistance in the stored grain weevils, *Sitophilus* spp. Sci Rep 2018;8:16361. <https://doi.org/10.1038/s41598-018-34513-5>.
212. Blanton AG, Peterson BF. Symbiont-mediated insecticide detoxification as an emerging problem in insect pests. Front Microbiol 2020;11. <https://doi.org/10.3389/fmicb.2020.547108>.
213. Carey AF, Carlson JR. Insect olfaction from model systems to disease control. Proc Natl Acad Sci U S A 2011;108:12987–95. <https://doi.org/10.1073/pnas.1103472108>.
214. Andersson MN, Newcomb RD. Pest control compounds targeting insect chemoreceptors: Another silent spring? Front Ecol Evol 2017;5. <https://doi.org/10.3389/fevo.2017.00005>.
215. Leal WS. Odorant reception in insects: roles of receptors, binding proteins, and degrading enzymes. Annu Rev Entomol 2013;58:373–91. <https://doi.org/10.1146/annurev-ento-120811-153635>.
216. Hassanali A, Herren H, Khan Z, Pickett J, Woodcock C. Integrated pest management: The push-pull approach for controlling insect pests and weeds of cereals, and its potential for other agricultural systems including animal husbandry. Philos Trans R Soc Lond B Biol Sci 2008;363:611–21. <https://doi.org/10.1098/rstb.2007.2173>.
217. Hatano E, Saveer AM, Borrero-Echeverry F, Strauch M, Zakir A, Bengtsson M, et al. A herbivore-induced plant volatile interferes with host plant and mate location in moths through suppression of olfactory signalling pathways. BMC Biol 2015;13:75.

- <https://doi.org/10.1186/s12915-015-0188-3>.
218. Ukeh DA, Woodcock CM, Pickett JA, Birkett MA. Identification of host kairomones from maize, *Zea mays*, for the maize weevil, *Sitophilus zeamais*. J Chem Ecol 2012;38:1402–9. <https://doi.org/10.1007/s10886-012-0191-x>.
219. Germinara GS, De Cristofaro A, Rotundo G. Behavioral responses of adult *Sitophilus granarius* to individual cereal volatiles. J Chem Ecol 2008;34:523–9. <https://doi.org/10.1007/s10886-008-9454-y>.
220. Phillips JK, Walgenbach CA, Klein JA, Burkholder WE, Schmuff NR, Fales HM. (R (*),S (*))-5-hydroxy-4-methyl-3-heptanone male-produced aggregation pheromone of *Sitophilus oryzae* (L.) and *S. zeamais* Motsch. J Chem Ecol 1985;11:1263–74. <https://doi.org/10.1007/BF01024114>.
221. Schmuff NR, Phillips JK, Burkholder WE, Fales HM, Chen C-W, Roller PP, et al. The chemical identification of the rice weevil and maize weevil aggregation pheromone. Tetrahedron Lett 1984;25:1533–4. [https://doi.org/10.1016/S0040-4039\(01\)90002-4](https://doi.org/10.1016/S0040-4039(01)90002-4).
222. Mitchell RF, Schneider TM, Schwartz AM, Andersson MN, McKenna DD. The diversity and evolution of odorant receptors in beetles (Coleoptera). Insect Mol Biol 2020;29:77–91. <https://doi.org/10.1111/imb.12611>.
223. de Bruyne M, Baker TC. Odor detection in insects: volatile codes. J Chem Ecol 2008;34:882–97. <https://doi.org/10.1007/s10886-008-9485-4>.
224. Benton R, Sachse S, Michnick SW, Vosshall LB. Atypical membrane topology and heteromeric function of *Drosophila* odorant receptors in vivo. PLoS Biol 2006;4:e20. <https://doi.org/10.1371/journal.pbio.0040020>.
225. Brand P, Robertson HM, Lin W, Pothula R, Klingeman WE, Jurat-Fuentes JL, et al. The origin of the odorant receptor gene family in insects. ELife 2018;7. <https://doi.org/10.7554/eLife.38340>.
226. Montagné N, de Fouchier A, Newcomb RD, Jacquín-Joly E. Advances in the identification and characterization of olfactory receptors in insects. Prog Mol Biol Transl Sci 2015;130:55–80. <https://doi.org/10.1016/bs.pmbts.2014.11.003>.
227. Mansourian S, Stensmyr MC. The chemical ecology of the fly. Curr Opin Neurobiol 2015;34:95–102. <https://doi.org/10.1016/j.conb.2015.02.006>.
228. Carey AF, Wang G, Su C-Y, Zwiebel LJ, Carlson JR. Odorant reception in the malaria mosquito *Anopheles gambiae*. Nature 2010;464:66–71. <https://doi.org/10.1038/nature08834>.
229. Wang G, Carey AF, Carlson JR, Zwiebel LJ. Molecular basis of odor coding in the malaria vector mosquito *Anopheles gambiae*. Proc Natl Acad Sci U S A 2010;107:4418–23. <https://doi.org/10.1073/pnas.0913392107>.
230. de Fouchier A, Walker WB, Montagné N, Steiner C, Binyameen M, Schlyter F, et al. Functional evolution of Lepidoptera olfactory receptors revealed by deorphanization of a moth repertoire. Nat Commun 2017;8:15709. <https://doi.org/10.1038/ncomms15709>.
231. Guo M, Du L, Chen Q, Feng Y, Zhang J, Zhang X, et al. Odorant receptors for detecting flowering plant cues are functionally conserved across moths and butterflies. Mol Biol Evol 2020. <https://doi.org/10.1093/molbev/msaa300>.
232. Pask GM, Slone JD, Millar JG, Das P, Moreira JA, Zhou X, et al. Specialized odorant receptors in social insects that detect cuticular hydrocarbon cues and candidate pheromones. Nat Commun 2017;8:297. <https://doi.org/10.1038/s41467-017-00099-1>.
233. Slone JD, Pask GM, Ferguson ST, Millar JG, Berger SL, Reinberg D, et al. Functional characterization of odorant receptors in the ponerine ant, *Harpegnathos saltator*. Proc Natl Acad Sci U S A 2017;114:8586–91. <https://doi.org/10.1073/pnas.1704647114>.
234. Mitchell RF, Hughes DT, Luetje CW, Millar JG, Soriano-Agatón F, Hanks LM, et al. Sequencing and characterizing odorant receptors of the cerambycid beetle *Megacyllene caryae*. Insect Biochem Mol Biol 2012;42:499–505. <https://doi.org/10.1016/j.ibmb.2012.03.007>.
235. Yuvaraj J, Roberts R, Sonntag Y, Hou X, Grosse-Wilde E, Machara A, et al. Putative ligand binding sites of two functionally characterized bark beetle odorant receptors. BMC Biol. 2021; 19:16. <https://doi.org/10.1101/2020.03.07.980797>.

236. Antony B, Johnny J, Montagné N, Jacquin-Joly E, Capoduro R, Cali K, et al. Pheromone receptor of the globally invasive quarantine pest of the palm tree, the red palm weevil (*Rhynchophorus ferrugineus*). *Mol Ecol* 2021;30(9):2025-2039 <https://doi.org/10.1111/mec.15874>.
237. Keller O, Odrionitz F, Stanke M, Kollmar M, Waack S. Scipio: using protein sequences to determine the precise exon/intron structures of genes and their orthologs in closely related species. *BMC Bioinformatics* 2008;9:278. <https://doi.org/10.1186/1471-2105-9-278>.
238. Slater GSC, Birney E. Automated generation of heuristics for biological sequence comparison. *BMC Bioinformatics* 2005;6:31. <https://doi.org/10.1186/1471-2105-6-31>.
239. Birney E, Clamp M, Durbin R. GeneWise and Genomewise. *Genome Res* 2004;14:988–95. <https://doi.org/10.1101/gr.1865504>.
240. Guindon S, Dufayard J-F, Lefort V, Anisimova M, Hordijk W, Gascuel O. New algorithms and methods to estimate maximum-likelihood phylogenies: assessing the performance of PhyML 3.0. *Syst Biol* 2010;59:307–21. <https://doi.org/10.1093/sysbio/syq010>.
241. Lefort V, Longueville J-E, Gascuel O. SMS: Smart Model Selection in PhyML. *Mol Biol Evol* 2017;34:2422–4. <https://doi.org/10.1093/molbev/msx149>.
242. Anisimova M, Gascuel O. Approximate likelihood-ratio test for branches: A fast, accurate, and powerful alternative. *Syst Biol* 2006;55:539–52. <https://doi.org/10.1080/10635150600755453>.
243. Makalowski W, Gotea V, Pande A, Makalowska I. Transposable elements: Classification, identification, and their use as a tool for comparative genomics. In: Anisimova M, editor. *Evol. Genomics Stat. Comput. Methods*, New York, NY: Springer; 2019, p. 177–207. https://doi.org/10.1007/978-1-4939-9074-0_6.
244. Flynn JM, Hubley R, Goubert C, Rosen J, Clark AG, Feschotte C, et al. RepeatModeler2 for automated genomic discovery of transposable element families. *Proc Natl Acad Sci U S A* 2020;117:9451–7. <https://doi.org/10.1073/pnas.1921046117>.
245. Ou S, Su W, Liao Y, Chougule K, Agda JRA, Hellinga AJ, et al. Benchmarking transposable element annotation methods for creation of a streamlined, comprehensive pipeline. *Genome Biol* 2019;20:275. <https://doi.org/10.1186/s13059-019-1905-y>.
246. Hernandez-Hernandez EM, Fernández-Medina RD, Navarro-Escalante L, Nuñez J, Benavides-Machado P, Carareto CMA. Genome-wide analysis of transposable elements in the coffee berry borer *Hypothenemus hampei* (Coleoptera: Curculionidae): description of novel families. *Mol Genet Genomics* 2017;292:565–83. <https://doi.org/10.1007/s00438-017-1291-7>.
247. Amorin I, Melo E, Moura R, Wallau G. Diverse mobilome of *Dichotomius* (*Luederwaldtinia*) *schiffleri* (Coleoptera: Scarabaeidae) reveals long-range horizontal transfer events of DNA transposons. *Mol Genet Genomics* 2020. <https://doi.org/10.1007/s00438-020-01703-8>.
248. Feschotte C, Zhang X, Wessler SR. Miniature inverted-repeat transposable elements and their relationship to established DNA transposons. *Mob DNA II* 2002:1147–58. <https://doi.org/10.1128/9781555817954.ch50>.
249. Feschotte C, Mouchès C. Recent amplification of miniature inverted-repeat transposable elements in the vector mosquito *Culex pipiens*: characterization of the Mimo family. *Gene* 2000;250:109–16. [https://doi.org/10.1016/S0378-1119\(00\)00187-6](https://doi.org/10.1016/S0378-1119(00)00187-6).
250. Feschotte C, Swamy L, Wessler SR. Genome-wide analysis of mariner-like transposable elements in rice reveals complex relationships with stowaway miniature inverted repeat transposable elements (MITEs). *Genetics* 2003;163:747–58.
251. Lu C, Chen J, Zhang Y, Hu Q, Su W, Kuang H. Miniature inverted-repeat transposable elements (MITEs) have been accumulated through amplification bursts and play important roles in gene expression and species diversity in *Oryza sativa*. *Mol Biol Evol*

- 2012;29:1005–17. <https://doi.org/10.1093/molbev/msr282>.
252. Feng Y. Plant MITEs: Useful tools for plant genetics and genomics. *Genomics Proteomics Bioinformatics* 2003;1:90–100. [https://doi.org/10.1016/S1672-0229\(03\)01013-1](https://doi.org/10.1016/S1672-0229(03)01013-1).
253. Sela N, Kim E, Ast G. The role of transposable elements in the evolution of non-mammalian vertebrates and invertebrates. *Genome Biol* 2010;11:R59. <https://doi.org/10.1186/gb-2010-11-6-r59>.
254. Petrov DA. DNA loss and evolution of genome size in *Drosophila*. *Genetica*. 2002 May;115(1):81-91.
255. Petrov DA, Hartl DL. High rate of DNA loss in the *Drosophila melanogaster* and *Drosophila virilis* species groups. *Mol Biol Evol* 1998;15:293–302. <https://doi.org/10.1093/oxfordjournals.molbev.a025926>.
256. Pasyukova EG, Nuzhdin SV. Doc and copia instability in an isogenic *Drosophila melanogaster* stock. *Mol Gen Genet MGG* 1993;240:302–6. <https://doi.org/10.1007/BF00277071>.
257. Ashburner M, Bergman CM. *Drosophila melanogaster*: a case study of a model genomic sequence and its consequences. *Genome Res* 2005;15:1661–7. <https://doi.org/10.1101/gr.3726705>.
258. Czech B, Hannon GJ. One loop to rule them all: The Ping-Pong cycle and piRNA-guided silencing. *Trends Biochem Sci* 2016;41:324–37. <https://doi.org/10.1016/j.tibs.2015.12.008>.
259. Sienski G, Dönertas D, Brennecke J. Transcriptional silencing of transposons by Piwi and Maelstrom and its impact on chromatin state and gene expression. *Cell* 2012;151:964–80. <https://doi.org/10.1016/j.cell.2012.10.040>.
260. Andersen PR, Tirian L, Vunjak M, Brennecke J. A heterochromatin-dependent transcription machinery drives piRNA expression. *Nature* 2017;549:54–9. <https://doi.org/10.1038/nature23482>.
261. Slotkin RK, Martienssen R. Transposable elements and the epigenetic regulation of the genome. *Nat Rev Genet* 2007;8:272–85. <https://doi.org/10.1038/nrg2072>.
262. Bewick AJ, Vogel KJ, Moore AJ, Schmitz RJ. Evolution of DNA Methylation across Insects. *Mol Biol Evol* 2017;34:654–65. <https://doi.org/10.1093/molbev/msw264>.
263. Ninova M, Griffiths-Jones S, Ronshaugen M. Abundant expression of somatic transposon-derived piRNAs throughout *Tribolium castaneum* embryogenesis. *Genome Biol* 2017;18:184. <https://doi.org/10.1186/s13059-017-1304-1>.
264. Mongelli V, Saleh M-C. Bugs are not to be silenced: Small RNA pathways and antiviral responses in insects. *Annu Rev Virol* 2016;3:573–89. <https://doi.org/10.1146/annurev-virology-110615-042447>.
265. Chambeyron S, Seitz H. Insect small non-coding RNA involved in epigenetic regulations. *Curr Opin Insect Sci* 2014;1:1–9. <https://doi.org/10.1016/j.cois.2014.05.001>.
266. Ishizu H, Siomi H, Siomi MC. Biology of PIWI-interacting RNAs: new insights into biogenesis and function inside and outside of germlines. *Genes Dev* 2012;26:2361–73. <https://doi.org/10.1101/gad.203786.112>.
267. Lewis SH, Quarles KA, Yang Y, Tanguy M, Frézal L, Smith SA, et al. Pan-arthropod analysis reveals somatic piRNAs as an ancestral defence against transposable elements. *Nat Ecol Evol* 2018;2:174–81. <https://doi.org/10.1038/s41559-017-0403-4>.
268. Guan D-L, Ding R-R, Hu X-Y, Yang X-R, Xu S-Q, Gu W, et al. Cadmium-induced genome-wide DNA methylation changes in growth and oxidative metabolism in *Drosophila melanogaster*. *BMC Genomics* 2019;20:356. <https://doi.org/10.1186/s12864-019-5688-z>.
269. Provataris P, Meusemann K, Niehuis O, Grath S, Misof B. Signatures of DNA methylation across insects suggest reduced DNA methylation levels in Holometabola. *Genome Biol Evol* 2018;10:1185–97. <https://doi.org/10.1093/gbe/evy066>.
270. Cunningham CB, Ji L, Wiberg RAW, Shelton J, McKinney EC, Parker DJ, et al. The genome and methylome of a beetle with complex social behavior, *Nicrophorus*

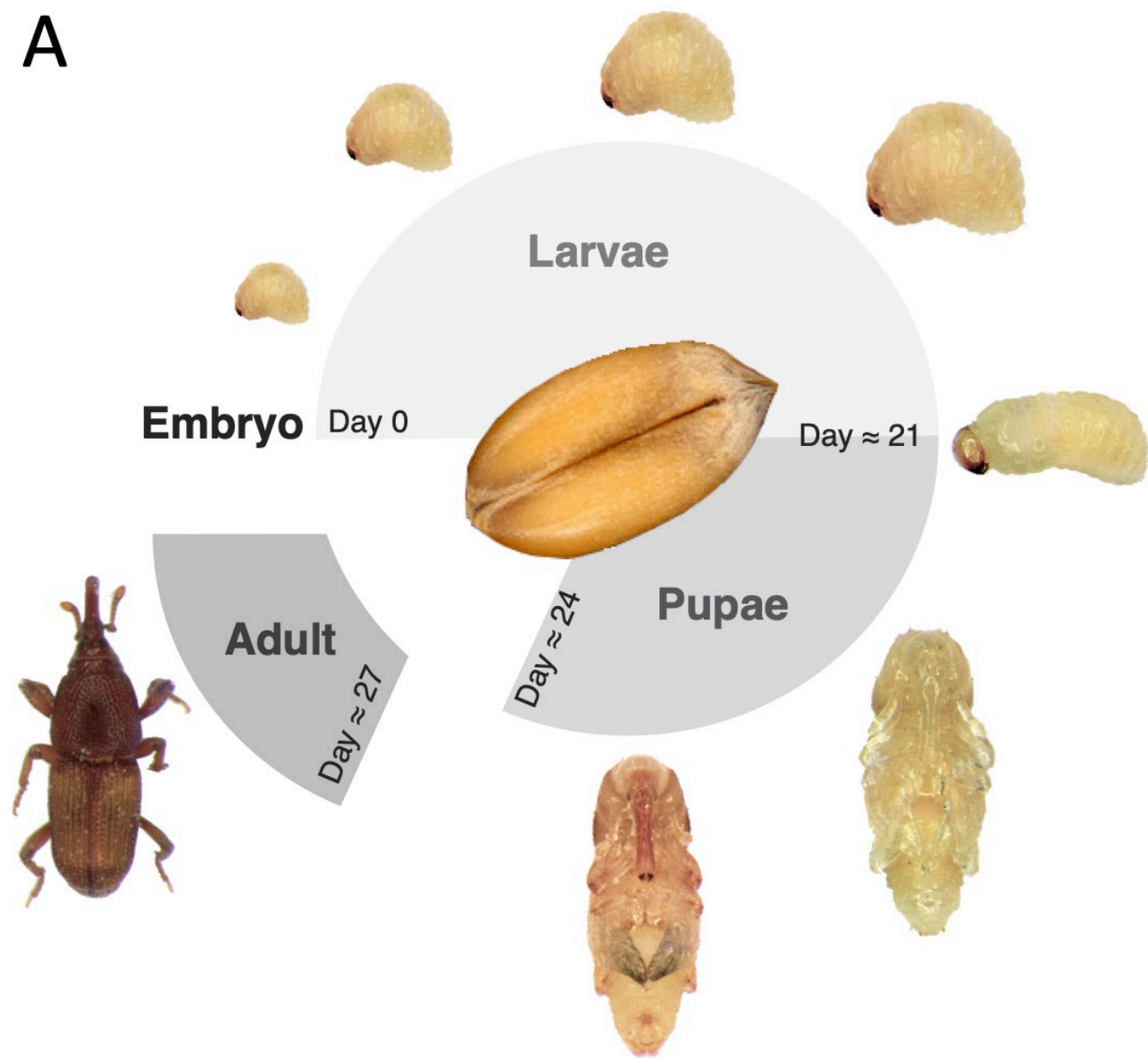
- vespillioides* (Coleoptera: Silphidae). *Genome Biol Evol* 2015;7:3383–96. <https://doi.org/10.1093/gbe/evv194>.
271. Tahiliani M, Koh KP, Shen Y, Pastor WA, Bandukwala H, Brudno Y, et al. Conversion of 5-methylcytosine to 5-hydroxymethylcytosine in mammalian DNA by MLL partner TET1. *Science* 2009;324:930–5. <https://doi.org/10.1126/science.1170116>.
272. Yao B, Li Y, Wang Z, Chen L, Poidevin M, Zhang C, et al. Active N6-methyladenine demethylation by DMAD regulates gene expression by coordinating with Polycomb protein in neurons. *Mol Cell* 2018;71:848–857.e6. <https://doi.org/10.1016/j.molcel.2018.07.005>.
273. Bestor TH, Holliday R, Monk M, Pugh JE. DNA methylation: evolution of a bacterial immune function into a regulator of gene expression and genome structure in higher eukaryotes. *Philos Trans R Soc Lond B Biol Sci* 1990;326:179–87. <https://doi.org/10.1098/rstb.1990.0002>.
274. Martienssen R. Transposons, DNA methylation and gene control. *Trends Genet* 1998;14:263–4. [https://doi.org/10.1016/S0168-9525\(98\)01518-2](https://doi.org/10.1016/S0168-9525(98)01518-2).
275. Zamudio N, Bourc'his D. Transposable elements in the mammalian germline: a comfortable niche or a deadly trap? *Heredity* 2010;105:92–104. <https://doi.org/10.1038/hdy.2010.53>.
276. Krueger F, Andrews SR. Bismark: a flexible aligner and methylation caller for Bisulfite-Seq applications. *Bioinformatics* 2011;27:1571–2. <https://doi.org/10.1093/bioinformatics/btr167>.
277. Langmead B, Salzberg SL. Fast gapped-read alignment with Bowtie 2. *Nat Methods* 2012;9:357–9. <https://doi.org/10.1038/nmeth.1923>.
278. Ramírez F, Ryan DP, Grüning B, Bhardwaj V, Kilpert F, Richter AS, et al. deepTools2: a next generation web server for deep-sequencing data analysis. *Nucleic Acids Res* 2016;44:W160–5. <https://doi.org/10.1093/nar/gkw257>.
279. Quinlan AR, Hall IM. BEDTools: a flexible suite of utilities for comparing genomic features. *Bioinformatics* 2010;26:841–2. <https://doi.org/10.1093/bioinformatics/btq033>.
280. Hill PWS, Amouroux R, Hajkova P. DNA demethylation, Tet proteins and 5-hydroxymethylcytosine in epigenetic reprogramming: an emerging complex story. *Genomics* 2014;104:324–33. <https://doi.org/10.1016/j.ygeno.2014.08.012>.
281. Wojciechowski M, Rafalski D, Kucharski R, Misztal K, Maleszka J, Bochtler M, et al. Insights into DNA hydroxymethylation in the honeybee from in-depth analyses of TET dioxygenase. *Open Biol* 2014;4. <https://doi.org/10.1098/rsob.140110>.
282. Zhang G, Huang H, Liu D, Cheng Y, Liu X, Zhang W, et al. N6-methyladenine DNA modification in *Drosophila*. *Cell* 2015;161:893–906. <https://doi.org/10.1016/j.cell.2015.04.018>.
283. Li-Byarlay H. The function of DNA methylation marks in social insects. *Front Ecol Evol* 2016;4. <https://doi.org/10.3389/fevo.2016.00057>.
284. Chamorro ML, Medeiros BAS de, Farrell BD. First phylogenetic analysis of Dryophthorinae (Coleoptera, Curculionidae) based on structural alignment of ribosomal DNA reveals Cenozoic diversification. *Ecol Evol* 2021;11:1984–98. <https://doi.org/10.1002/ece3.7131>.
285. Lynch M, Conery JS. The origins of genome complexity. *Science* 2003;302:1401–4. <https://doi.org/10.1126/science.1089370>.
286. Peona V, Blom MPK, Xu L, Burri R, Sullivan S, Bunikis I, et al. Identifying the causes and consequences of assembly gaps using a multiplatform genome assembly of a bird-of-paradise. *Mol Ecol Resour*. 2021;21(1):263–286. <https://doi.org/10.1111/1755-0998.13252>.
287. Di Genova A, Buena-Atienza E, Ossowski S, Sagot M-F. Efficient hybrid *de novo* assembly of human genomes with WENGAN. *Nat Biotechnol* 2020;1–9. <https://doi.org/10.1038/s41587-020-00747-w>.
288. Platt RN II, Blanco-Berdugo L, Ray DA. Accurate transposable element annotation is vital when analyzing new genome assemblies. *Genome Biol Evol* 2016;8:403–10. <https://doi.org/10.1093/gbe/evw009>.

289. Maire J, Parisot N, Galvao Ferrarini M, Vallier A, Gillet B, Hughes S, et al. Spatial and morphological reorganization of endosymbiosis during metamorphosis accommodates adult metabolic requirements in a weevil. *Proc Natl Acad Sci U S A* 2020;117:19347–58.
290. Nardon P. Obtention d'une souche asymbiotique chez le charançon *Sitophilus sasakii* Tak: différentes méthodes d'obtention et comparaison avec la souche symbiotique d'origine. *CR Acad Sci Paris D* 1973;277:981–4.
291. Li H. BFC: correcting Illumina sequencing errors. *Bioinformatics* 2015;31:2885–7. <https://doi.org/10.1093/bioinformatics/btv290>.
292. Salmela L, Rivals E. LoRDEC: accurate and efficient long read error correction. *Bioinformatics* 2014;30:3506–14. <https://doi.org/10.1093/bioinformatics/btu538>.
293. Magoc T, Salzberg SL. FLASH: fast length adjustment of short reads to improve genome assemblies. *Bioinformatics* 2011;27:2957–63. <https://doi.org/10.1093/bioinformatics/btr507>.
294. Chikhi R, Rizk G. Space-efficient and exact de Bruijn graph representation based on a Bloom filter. *Algorithms Mol Biol.* 2013;8(1):22.
295. Walker BJ, Abeel T, Shea T, Priest M, Abouelliel A, Sakthikumar S, et al. Pilon: An integrated tool for comprehensive microbial variant detection and genome assembly improvement. *PLoS One* 2014;9:e112963. <https://doi.org/10.1371/journal.pone.0112963>.
296. Di Genova A, Ruz GA, Sagot M-F, Maass A. Fast-SG: an alignment-free algorithm for hybrid assembly. *GigaScience* 2018;7. <https://doi.org/10.1093/gigascience/giy048>.
297. Mandric I, Zelikovsky A. ScaffoldMatch: scaffolding algorithm based on maximum weight matching. *Bioinformatics* 2015;31:2632–8. <https://doi.org/10.1093/bioinformatics/btv211>.
298. Xu G-C, Xu T-J, Zhu R, Zhang Y, Li S-Q, Wang H-W, et al. LR_Gapcloser: a tiling path-based gap closer that uses long reads to complete genome assembly. *GigaScience* 2019;8. <https://doi.org/10.1093/gigascience/giy157>.
299. Song L, Shankar DS, Florea L. Rascaf: Improving genome assembly with RNA sequencing data. *Plant Genome* 2016;9:1–12. <https://doi.org/10.3835/plantgenome2016.03.0027>.
300. Paulino D, Warren RL, Vandervalk BP, Raymond A, Jackman SD, Birol I. Sealer: a scalable gap-closing application for finishing draft genomes. *BMC Bioinformatics* 2015;16:230. <https://doi.org/10.1186/s12859-015-0663-4>.
301. Roach MJ, Schmidt SA, Borneman AR. Purge Haplotigs: allelic contig reassignment for third-gen diploid genome assemblies. *BMC Bioinformatics* 2018;19:460. <https://doi.org/10.1186/s12859-018-2485-7>.
302. Guan D, McCarthy SA, Wood J, Howe K, Wang Y, Durbin R. Identifying and removing haplotypic duplication in primary genome assemblies. *Bioinformatics* 2020;36:2896–8. <https://doi.org/10.1093/bioinformatics/btaa025>.
303. Mikheenko A, Prjibelski A, Saveliev V, Antipov D, Gurevich A. Versatile genome assembly evaluation with QUAST-LG. *Bioinformatics* 2018;34:i142–50. <https://doi.org/10.1093/bioinformatics/bty266>.
304. Kokot M, Długosz M, Deorowicz S. KMC 3: counting and manipulating k-mer statistics. *Bioinformatics* 2017;33:2759–61. <https://doi.org/10.1093/bioinformatics/btx304>.
305. Marçais G, Kingsford C. A fast, lock-free approach for efficient parallel counting of occurrences of k-mers. *Bioinformatics* 2011;27:764–70. <https://doi.org/10.1093/bioinformatics/btr011>.
306. Smit AF, Hubley R, Green P. RepeatMasker Open-4.0. <http://www.repeatmasker.org> 2013.
307. Crescente JM, Zavallo D, Helguera M, Vanzetti LS. MITE Tracker: an accurate approach to identify miniature inverted-repeat transposable elements in large genomes. *BMC Bioinformatics* 2018;19:348. <https://doi.org/10.1186/s12859-018-2376-y>.
308. Schloss PD, Westcott SL, Ryabin T, Hall JR, Hartmann M, Hollister EB, et al.

- Introducing mothur: Open-source, platform-independent, community-supported software for describing and comparing microbial communities. *Appl Environ Microbiol* 2009;75:7537–41. <https://doi.org/10.1128/AEM.01541-09>.
309. Novák P, Ávila Robledillo L, Koblížková A, Vrbová I, Neumann P, Macas J. TAREAN: a computational tool for identification and characterization of satellite DNA from unassembled short reads. *Nucleic Acids Res* 2017;45:e111. <https://doi.org/10.1093/nar/gkx257>.
310. Storer J, Hubley R, Rosen J, Wheeler TJ, Smit AF. The Dfam community resource of transposable element families, sequence models, and genome annotations. *Mob DNA* 2021;12:2. <https://doi.org/10.1186/s13100-020-00230-y>.
311. Storer JM, Hubley R, Rosen J, Smit AFA. Curation guidelines for *de novo* generated transposable element families. *Curr Protoc* 2021;1:e154. <https://doi.org/10.1002/cpz1.154>.
312. Bao W, Kojima KK, Kohany O. Repbase Update, a database of repetitive elements in eukaryotic genomes. *Mob DNA* 2015;6:11. <https://doi.org/10.1186/s13100-015-0041-9>.
313. Lu S, Wang J, Chitsaz F, Derbyshire MK, Geer RC, Gonzales NR, et al. CDD/SPARCLE: the conserved domain database in 2020. *Nucleic Acids Res* 2020;48:D265–8. <https://doi.org/10.1093/nar/gkz991>.
314. Kapusta A, Suh A. Evolution of bird genomes—a transposon’s-eye view. *Ann N Y Acad Sci* 2017;1389:164–85. <https://doi.org/10.1111/nyas.13295>.
315. Bolger AM, Lohse M, Usadel B. Trimmomatic: a flexible trimmer for Illumina sequence data. *Bioinformatics* 2014;30:2114–20. <https://doi.org/10.1093/bioinformatics/btu170>.
316. Dobin A, Davis CA, Schlesinger F, Drenkow J, Zaleski C, Jha S, et al. STAR: ultrafast universal RNA-seq aligner. *Bioinformatics* 2013;29:15–21. <https://doi.org/10.1093/bioinformatics/bts635>.
317. Liao Y, Smyth GK, Shi W. featureCounts: an efficient general purpose program for assigning sequence reads to genomic features. *Bioinformatics* 2014;30:923–30. <https://doi.org/10.1093/bioinformatics/btt656>.
318. Lerat E, Fablet M, Modolo L, Lopez-Maestre H, Vieira C. TETools facilitates big data expression analysis of transposable elements and reveals an antagonism between their activity and that of piRNA genes. *Nucleic Acids Res* 2017;45:e17. <https://doi.org/10.1093/nar/gkw953>.
319. Love MI, Huber W, Anders S. Moderated estimation of fold change and dispersion for RNA-seq data with DESeq2. *Genome Biol* 2014;15:550. <https://doi.org/10.1186/s13059-014-0550-8>.
320. *Sitophilus oryzae* breed Bouriz, whole genome shotgun sequencing project 2019.
321. Low coverage genome sequencing of maize weevil *Sitophilus zeamais* to analyse the repeatome. 2021.
322. Low coverage genome sequencing of granary weevil *Sitophilus granarius*. 2021.
323. Low coverage genome sequencing of the tamarind weevil *Sitophilus linearis*. 2021.
324. Rebollo R, Goubert C. Transposable element annotation of *Sitophilus oryzae* 2021. <https://doi.org/10.5281/zenodo.4570415>.
325. RNAseq of midgut and ovaries of Day 10 *Sitophilus oryzae* females. 2021.
326. DNA methylation in *Sitophilus oryzae* ovaries. 2021.
327. Misof B, Liu S, Meusemann K, Peters RS, Donath A, Mayer C, et al. Phylogenomics resolves the timing and pattern of insect evolution. *Science* 2014;346:763–7. <https://doi.org/10.1126/science.1257570>.

Figure 1

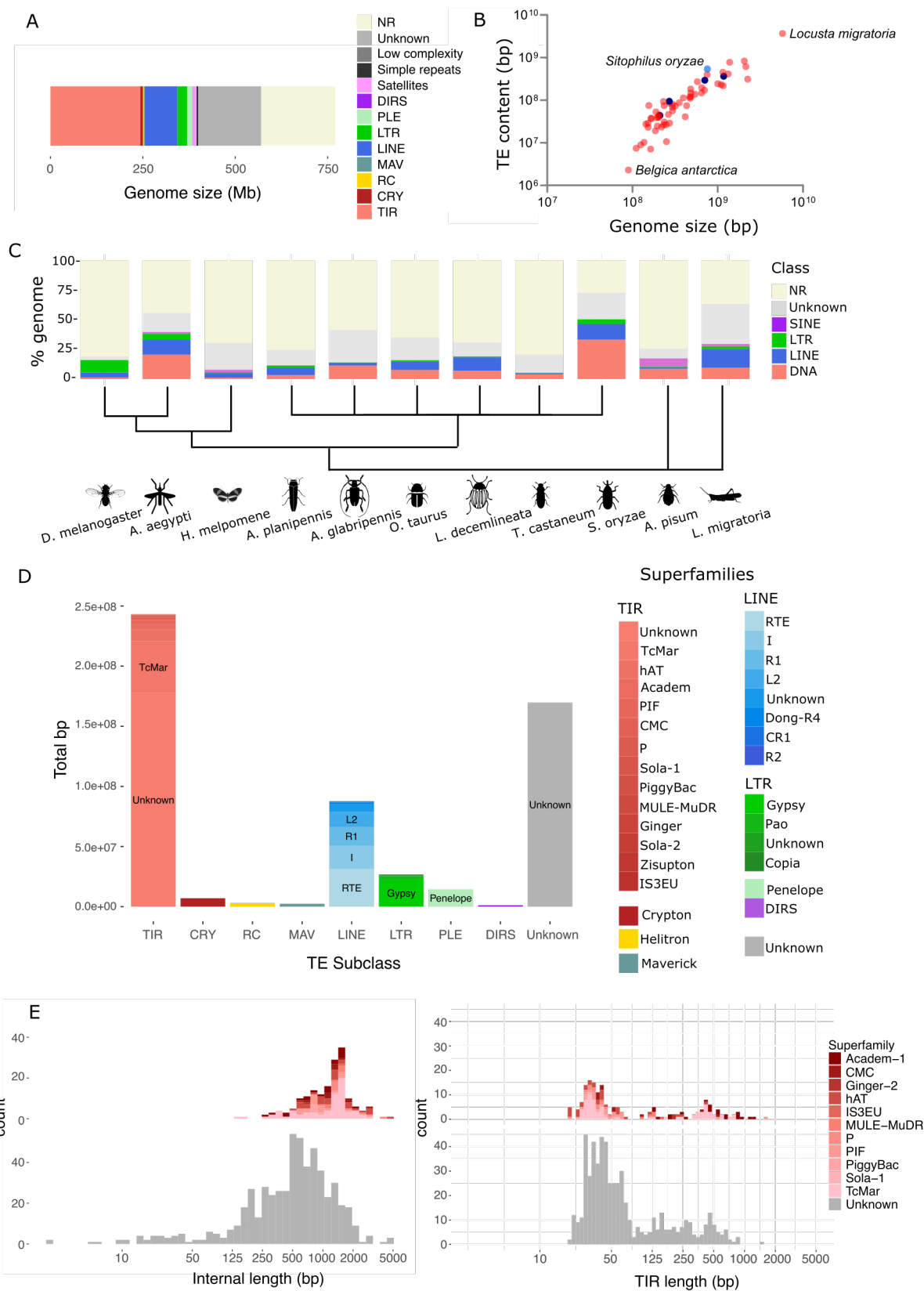
A



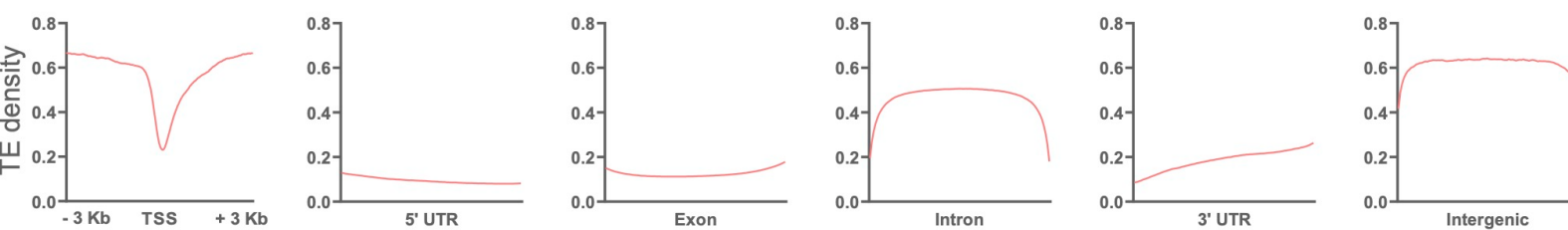
B



Figure 2



A



B

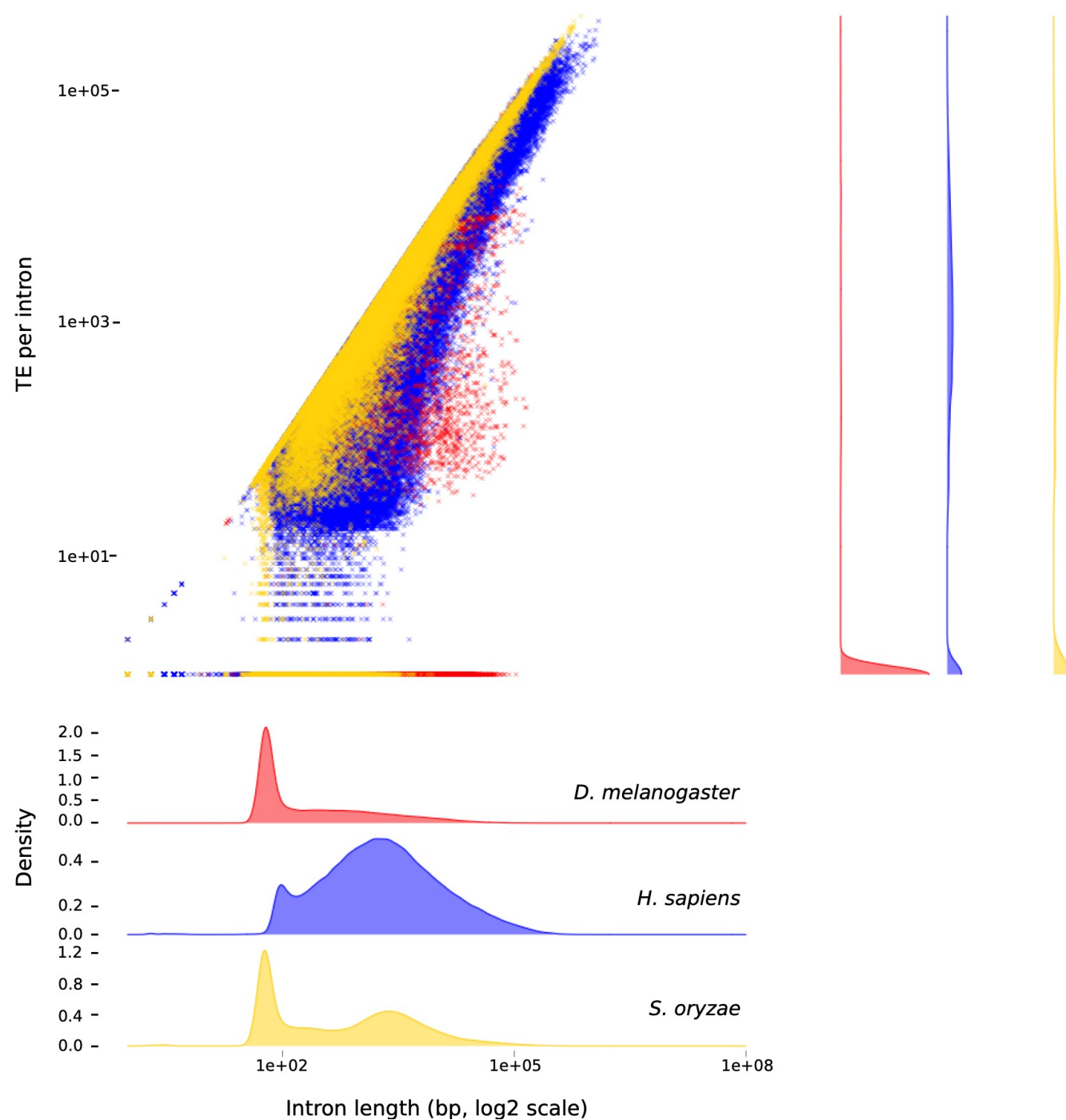
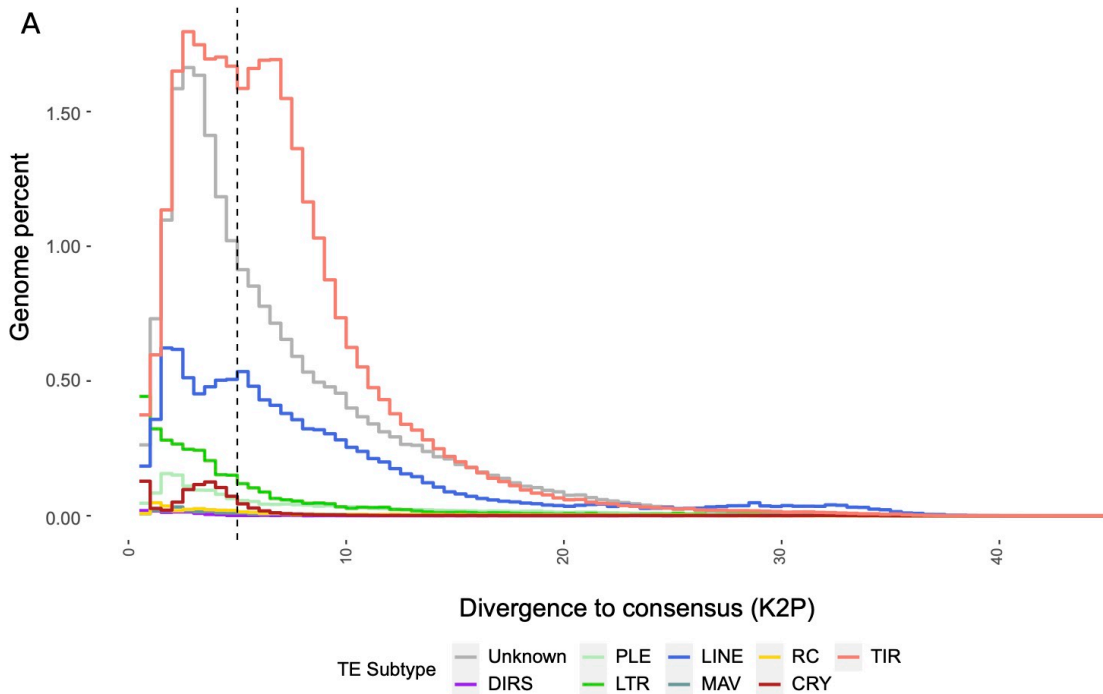


Figure 4



B

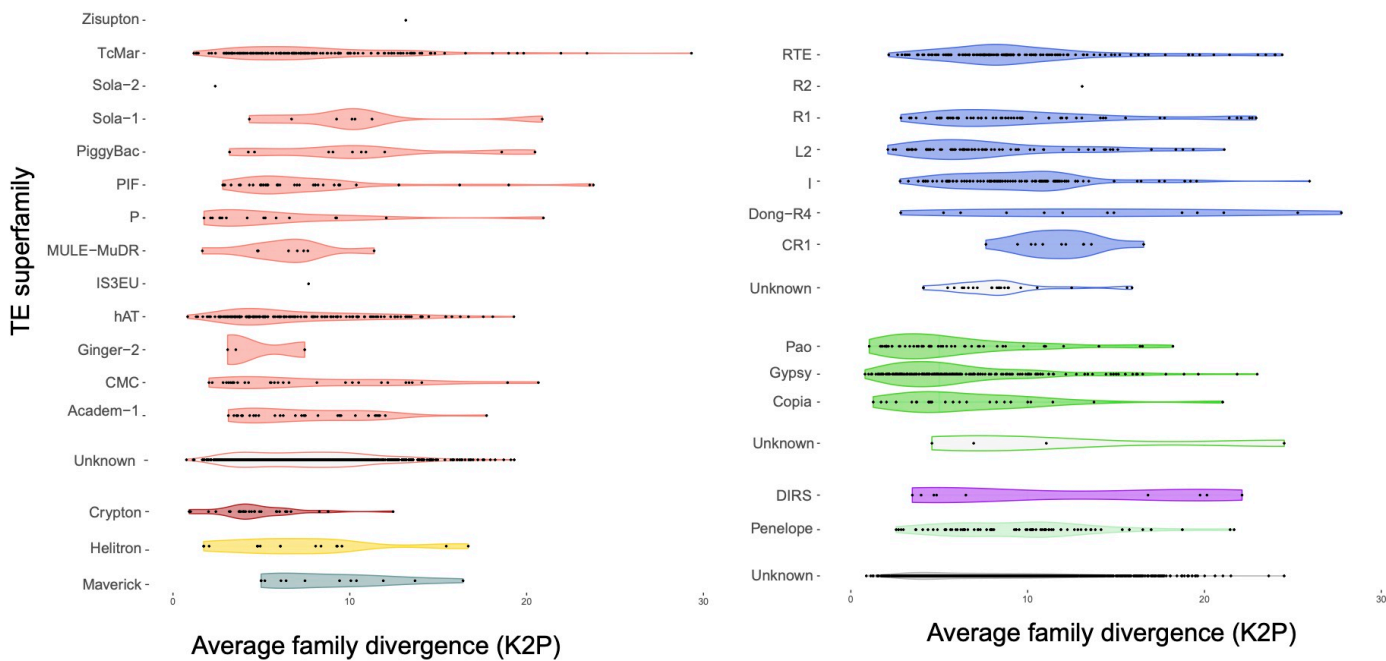
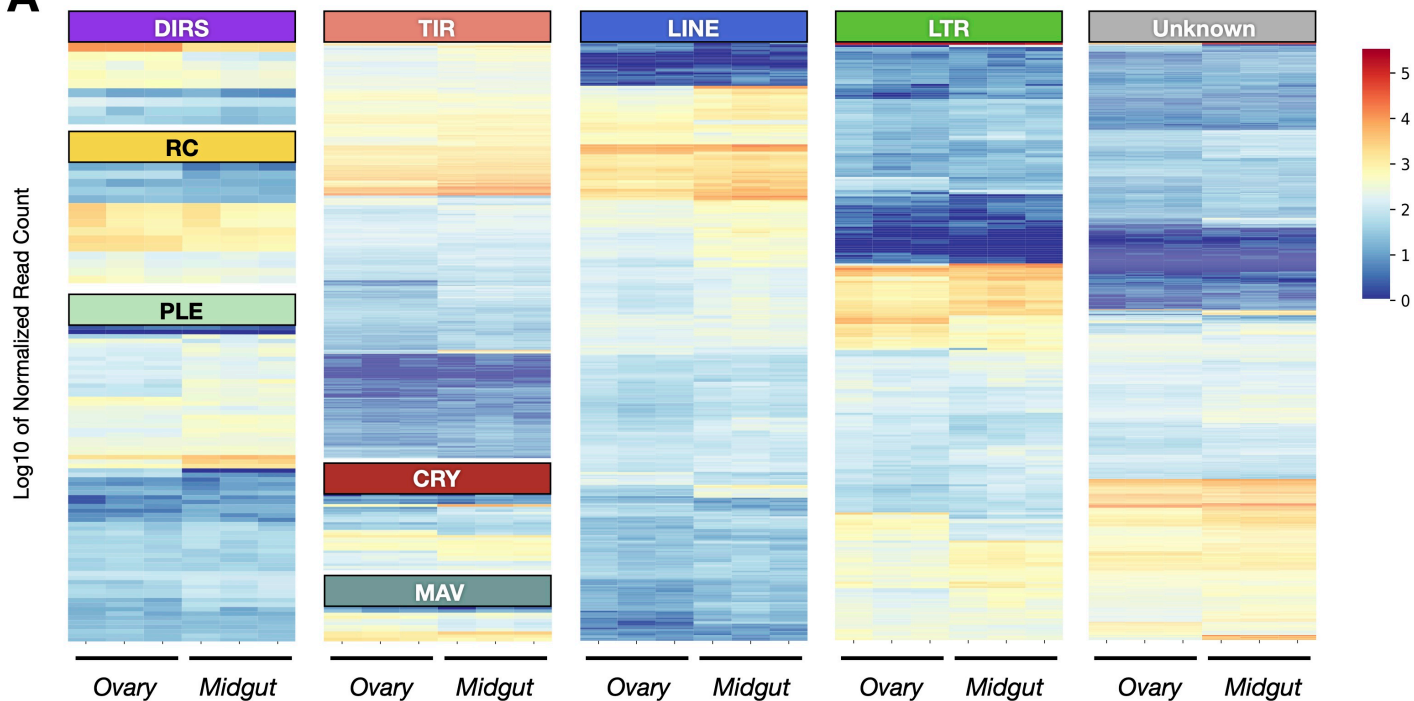
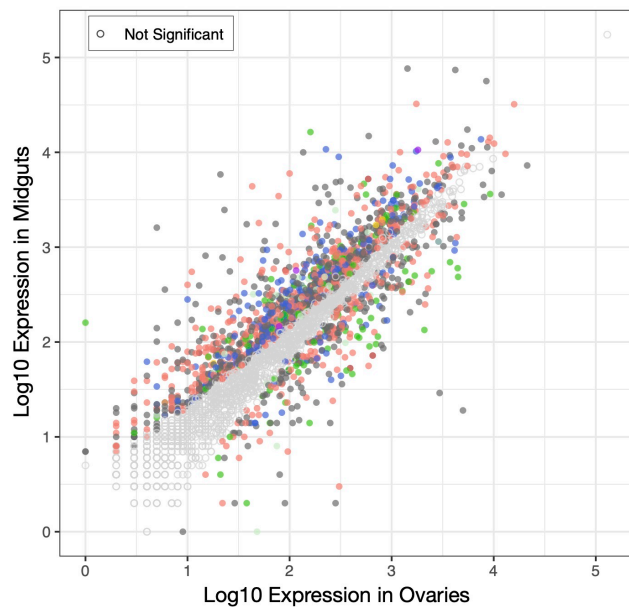


Figure 5

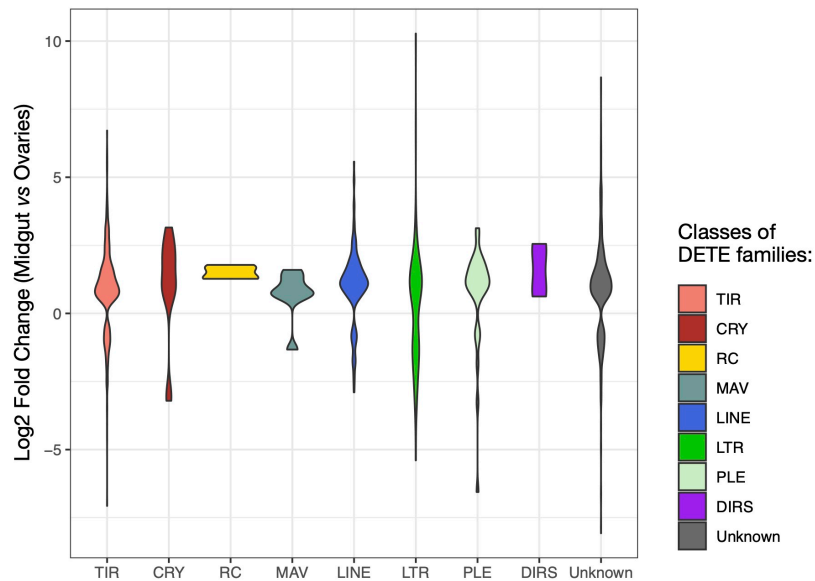
A



B



C



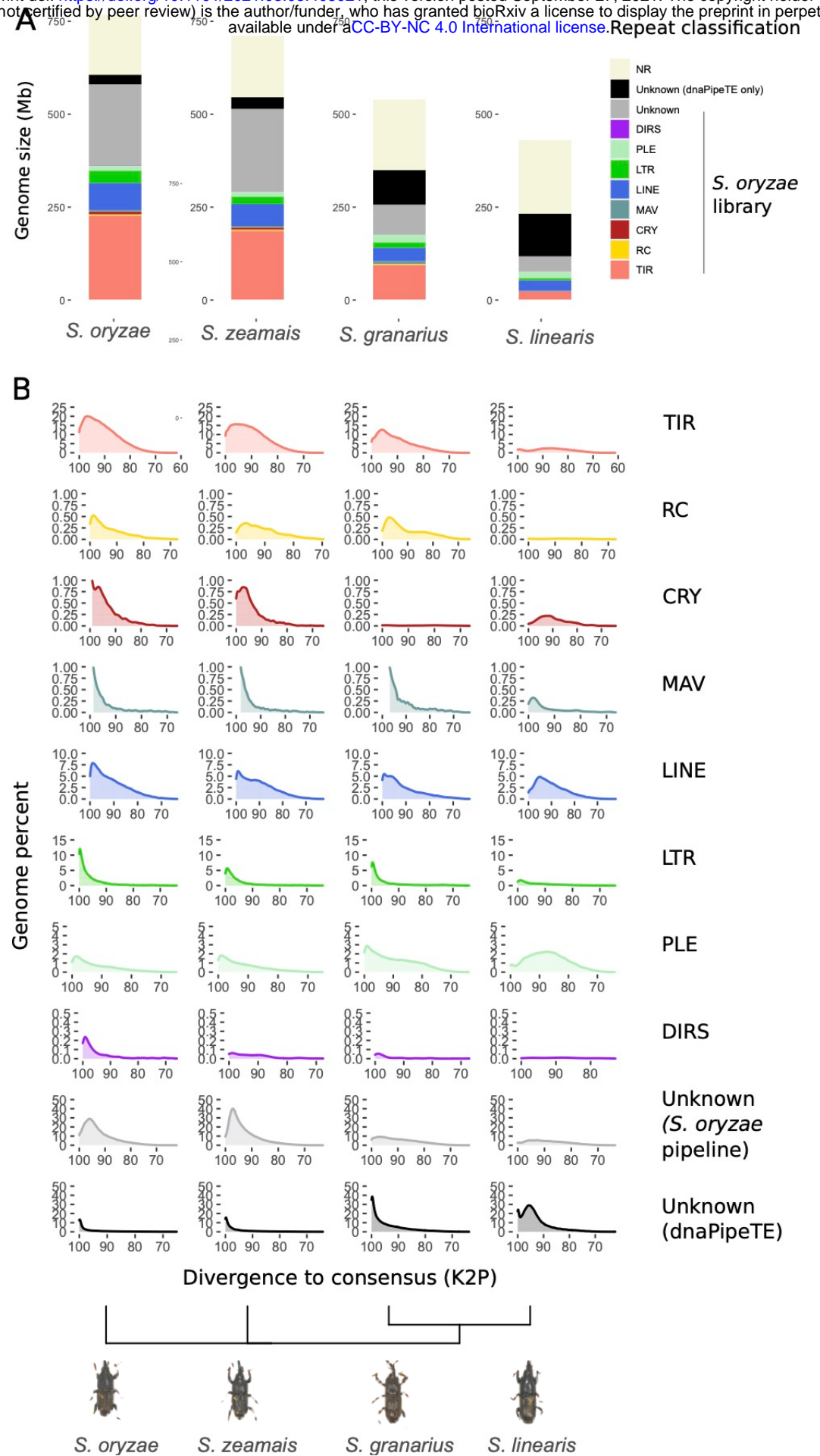


Figure 7

